IAEA-TECDOC-1597

Clinical Applications of SPECT/CT: New Hybrid Nuclear Medicine Imaging System

IAEA
International Atomic Energy Agency

August 2008

IAEA-TECDOC-1597

Clinical Applications of SPECT/CT: New Hybrid Nuclear Medicine Imaging System

IAEA
International Atomic Energy Agency

August 2008

The originating Section of this publication in the IAEA was:

Nuclear Medicine Section
International Atomic Energy Agency
Wagramer Strasse 5
P.O. Box 100
A-1400 Vienna, Austria

CLINICAL APPLICATIONS OF SPECT/CT:
NEW HYBRID NUCLEAR MEDICINE IMAGING SYSTEM

IAEA, VIENNA, 2008
IAEA-TECDOC-1597
ISBN 978-92-0-107108-8
ISSN 1011–4289

Printed by the IAEA in Austria
August 2008

FOREWORD

Interest in multimodality imaging shows no sign of subsiding. New tracers are spreading out the spectrum of clinical applications and innovative technological solutions are preparing the way for yet more modality marriages: hybrid imaging.

Single photon emission computed tomography (SPECT) has enabled the evaluation of disease processes based on functional and metabolic information of organs and cells. Integration of X ray computed tomography (CT) into SPECT has recently emerged as a brilliant diagnostic tool in medical imaging, where anatomical details may delineate functional and metabolic information.

SPECT/CT has proven to be valuable in oncology. For example, in the case of a patient with metastatic thyroid cancer, neither SPECT nor CT alone could identify the site of malignancy. SPECT/CT, a hybrid image, precisely identified where the surgeon should operate.

However SPECT/CT is not just advantageous in oncology. It may also be used as a one-stop-shop for various diseases.

Clinical applications with SPECT/CT have started and expanded in developed countries. It has been reported that moving from SPECT alone to SPECT/CT could change diagnoses in 30% of cases. Large numbers of people could therefore benefit from this shift all over the world.

This report presents an overview of clinical applications of SPECT/CT and a relevant source of information for nuclear medicine physicians, radiologists and clinical practitioners. This information may also be useful for decision making when allocating resources dedicated to the health care system, a critical issue that is especially important for the development of nuclear medicine in developing countries. In this regard, the IAEA may be heavily involved in the promotion of programmes aimed at the IAEA's coordinated research projects and Technical Cooperation projects.

The IAEA wishes to express its thanks to all experts who have contributed to this publication. The IAEA officer responsible for this publication was N. Watanabe of the Division of Human Health.

EDITORIAL NOTE

The use of particular designations of countries or territories does not imply any judgement by the publisher, the IAEA, as to the legal status of such countries or territories, of their authorities and institutions or of the delimitation of their boundaries.

The mention of names of specific companies or products (whether or not indicated as registered) does not imply any intention to infringe proprietary rights, nor should it be construed as an endorsement or recommendation on the part of the IAEA.

CONTENTS

1. INTRODUCTION

During the past several years there has been growing utilization of PET/CT, based on the fact that functional and morphologic correlative images produced by this methodology improve diagnostic accuracy. Similar progress is now being reported for SPECT/CT, a modality which is rapidly evolving from a somewhat under-utilized technical option to gain an acknowledged status for optimizing the diagnostic capabilities of single photon imaging, with potential impact on patient management.

SPECT and CT are tomographic imaging procedures, each one with separately proven good diagnostic performance. SPECT produces computer-generated images of local radiotracer uptake, while CT produces 3-D anatomic images of X ray density of the human body. Combined SPECT/CT imaging provides sequentially functional information from SPECT and the anatomic information from CT, obtained during a single examination. CT data are also used for rapid and optimal attenuation correction of the single photon emission data.

By precisely localizing areas of abnormal and/or physiological tracer uptake, SPECT/CT improves sensitivity and specificity, but can also aid in achieving accurate dosimetric estimates as well as in guiding interventional procedures or in better defining the target volume for external beam radiation therapy.

Gamma camera imaging with single photon emitting radiotracers represents the majority of procedures in a routine nuclear medicine practice. Many of these examinations are tumour or cardiac imaging studies. The development of better instruments, newer computer based procedures for image analysis and display, new ^{99m}Tc labelled agents for visualizing biologically significant events (such as cellular growth, hypoxia, angiogenesis, apoptosis) may enhance the future value of SPECT/CT in terms of both clinical impact on patient care and cost effectiveness, as compared to PET/CT.

Diagnosis and characterization of disease by CT imaging is based on morphologic criteria such as size, texture and tissue attenuation. CT provides information regarding changes in organ size and tissue density, as well as their precise spatial localization and topographic landmarks. However, structural data do not necessarily correlate with the metabolic status of disease. On the other hand, nuclear medicine imaging is based on the bio-distribution of a radioactive agent over time and space, thus visualizing dynamic physiological and pathophysiological processes that define the functional characteristics of disease. Furthermore, whole body assessment is possible with a single radiation exposure, as the ionizing agent is administered to patients rather than being delivered from an external source to each region of the body to be evaluated, as performed with radiologic imaging (e.g. conventional X ray or CT). However, scintigraphic images lack accurate anatomic landmarks for precise localization and characterization of findings, in spite of the fact that specific radiopharmaceuticals are used for assessment and diagnosis of specific disease processes. The above mentioned considerations explain why morphologic and functional imaging modalities are complementary and not competing techniques, especially if precise image registration is made possible by using a single imaging unit combining the emission based data (SPECT) with the transmission based data (CT, which also serve to correct the emission data for tissue attenuation). Image registration is the process of determining the geometric relationship between multimodality imaging studies, in order to use information provided by one test in the context of the other modality.

2. OVERVIEW OF SPECT/CT TECHNOLOGY

2.1. Update on SPECT/CT installations worldwide

While image fusion techniques have been in clinical use for many years, the first commercial SPECT/CT system was only introduced in 1999. This system combined a low-power X ray tube with separate gamma and X ray detectors mounted on the same slip ring gantry. The X ray system operated at 140 kV with a tube current of only 2.5 mA. This resulted in a significantly lower patient dose than that received during a conventional CT imaging procedure (by a factor of 4–5), but the quality of the CT images was inferior to state of the art CT. Nevertheless, the fan beam formed by the X ray tube on the detectors allowed the measurement of patient attenuation along discrete paths providing significantly higher quality attenuation maps than those available with conventional ^{153}Gd scanning lines sources [1, 2].

This system has recently been equipped with a 4 slice low-dose CT scanner yielding an axial slice thickness of 5 mm with each rotation instead of one 10 mm slice. This tool retains the very compact design of the previous system, delivers a low radiation dose to the patient and requires minimal room shielding [2, 3]. Over the last 2–3 years there has been a large expansion of SPECT/CT technology worldwide and, as at June 2007, there are approximately 600 of these installations around the world and over 200 across the United States. The relatively large distribution of these SPECT/CT systems equipped with a low definition CT tube versus those equipped with high definition, standard diagnostic CT tubes (see below) can be explained by two main factors: 1) this is the first SPECT/CT system made commercially available, and 2) the overall cost of these tomographs (equipped with a low definition CT component) is considerably lower than that of tomographs equipped with a CT component having full diagnostic capabilities.

In this regard, following the commercial success of PET/CT systems that employ multi-slice CT scanners, there has been growing interest in the development of comparable SPECT/CT systems. Thus, in an effort to further improve imaging quality and reduce acquisition time, new hybrid systems employing state of the art spiral CT scanners have been developed. These systems combine dual-head gamma cameras with full diagnostic, up to 16 slice CT scanners that allow variation of CT slice thickness from 0.6 mm up to 10 mm, yielding diagnostic quality CT images with a scan speed shorter than 30 s for a 40 cm axial field of view [2, 3]. However, because of the addition of a separate CT gantry, these systems are considerably larger than conventional SPECT systems and have very different setting and shielding requirements compared with the system equipped with the low definition CT tube. Since their introduction in the market, over 210 such units have been installed worldwide.

Access to hybrid systems is limited in several countries due to their high cost, SPECT/CT systems based on combining a ‘gantry-free’ commercial SPECT system with a single- or multiple-slice CT scanner have recently been developed [4, 5]. In the future, further cost reduction and technological improvement are desirable in order to encourage a larger diffusion of such devices worldwide.

2.2. General architecture of SPECT/CT devices

SPECT/CT systems have the same SPECT component as conventional nuclear medicine systems, the dual-head gamma cameras are generally used for planar and tomographic imaging of single photon emitting radiotracers. As mentioned above, the CT component of the first-generation hybrid devices used a low resolution CT detector while recently

developed, second-generation SPECT/CT systems incorporate a variety of multi-slice CT scanners. SPECT/CT systems include separate CT and gamma camera devices using common or adjacent mechanical gantries, and sharing the same scanning table. Integration of SPECT and X ray imaging data is performed by a process that is similar to that of PET/CT.

X ray scatter can reach and possibly damage the SPECT detectors designed for radionuclide low count rate imaging. Therefore, in a hybrid system the SPECT detectors are off-set in the axial direction from the plane of the X ray source and detector. In a hybrid system both detectors have to be able to rotate and position accurately for tomographic imaging. In this regard, accuracy of translation and angular motion differs from one imaging system to another. While CT requires the highest accuracy, SPECT (with a lower spatial resolution) can perform clinical images with a motion accuracy of slightly less than one millimetre.

SPECT/CT systems using a low-dose single- or multi-slice CT have both the SPECT and the CT detectors mounted on the same rotating platform. Imaging is performed while the detectors are rotating sequentially around the patient. While this concept has the advantage of using the gantry of a conventional gamma camera for both imaging modalities, it limits the rotational speed of the SPECT/CT option to approximately 20 seconds per rotation. In SPECT/CT systems incorporating diagnostic CT scanners, the gamma camera detectors are mounted on a different platform, separated from the high speed rotating CT device (0.25 to 0.5 s per revolution). This design increases the performance of the CT subsystem, but it also increases the complexity of the gantry and the cost of the technology.

Dual modality imaging requires longer stretchers than single modality imaging devices. While built to support patients weighing up to 500 pounds, these scanning tables, extended to accommodate the needs of both components (SPECT and CT), deflect to some degree while loaded with normal adult patients. The extension and degree of deflection of the table can introduce a patient-dependent mis-registration between CT and SPECT data. One solution to this problem is the design of a table supported on its base at the front of the scanner as well as at the far end of the X ray system, thus minimizing the table deflection. Another solution is to use a table fixed on a base, moving on the floor to introduce the patient into the scanner.

The workstation of the SPECT/CT device is responsible for system control, data acquisition, image reconstruction and display, as well as data processing and analysis. CT data are calibrated in order to obtain attenuation correction maps for the SPECT images. SPECT and CT images are displayed on the same screen in addition to the fused images, which represent the overlay of a coloured SPECT over a grey-scale CT image. A 3-D display with triangulation options allows to locate lesions and sites of interest on the CT image and to redisplay them on the registered SPECT and fused SPECT/CT images.

2.3. SPECT/CT acquisition protocols

Acquisition on SPECT/CT systems is performed in a sequential mode. With devices that have a low-dose CT component, data are typically acquired by rotating the X ray detector 220° around the patient, with the X ray tube operated at 140 kV and 2.5 mA. The CT images obtained have an in-plane spatial resolution of 2.5 mm, and of 10 mm in the axial direction. Scan time is approximately 16 s per slice, for a total study duration of 10 min for the CT. SPECT/CT systems using a diagnostic CT component are characterized by higher spatial resolution and faster scanning time (approximately 30 s for the whole field of view),

associated however with higher radiation doses. An attenuation map is created at the end of the CT acquisition time.

The SPECT component is represented by a rotating, dual-head, variable angle sodium-iodide scintillation camera. The detectors can be placed either in a 180° or a 90° position. Regardless of the type of SPECT/CT that is used, SPECT acquisition currently requires a routine scanning time of approximately 20–30 min, depending on the radiotracer, as for stand-alone SPECT acquisition protocols. SPECT is reconstructed using iterative methods incorporating photon attenuation correction based on the X ray transmission map and scatter correction.

Since X ray and radionuclide data are not acquired simultaneously, SPECT images are not contaminated by scatter radiation generated during the X ray image acquisition. Also, since the patient is not removed from the table, both imaging components are acquired with a consistent and identical patient position, allowing accurate image registration if we assume that the patient has not moved during the entire duration of the SPECT/CT study. CT is usually acquired in matrices of 512 × 512 with the newest CT scanners, or 256 × 256 in older scanners, and has to be resized into slices with the same pixel format and slice width as SPECT. Spatial registration of the CT and SPECT acquisitions is important since misalignment of the attenuation map relative to corresponding radionuclide images can cause ‘edge artefacts’, bright and dark ‘rims’ across edges of these regions.

SPECT/CT image mis-registration or blurring may occur, mainly due to patient movement as well as respiration, cardiac motion, and peristalsis. Differences in urinary bladder filling can lead to erroneous co-registration between SPECT and CT acquisitions. With SPECT/CT devices equipped with low-dose X ray tubes, CT is performed during shallow breathing to facilitate image registration. However, the longer acquisition time increases the chances for patient motion. With hybrid devices equipped with multi-slice CT, anatomic imaging is acquired following breath-hold, during tidal breathing, or during a short part of the respiratory cycle, whereas SPECT data are acquired over several minutes. This again can lead to mis-registration. In addition to faulty localization, non-registered attenuation maps can lead to under- or overestimation of radionuclide uptake.

The presence of contrast media in the CT images acquired as part of the SPECT/CT study complicates the attenuation correction process. Also, high concentrations of intra-venous contrast material captured during the CT acquisition may have redistributed by the time the SPECT acquisition is performed. Image segmentation techniques separating different areas inside the images may solve this problem, or alternatively, a very low powered non-contrast CT can be performed prior to the SPECT for attenuation correction, followed by the contrast CT study as the last step.

2.4. Technical staffing for SPECT/CT

A major asset for proper implementation of novel SPECT/CT procedures is the technologist. It is important to take the time to train and educate the technologists so that they can deliver an end product of the highest quality. While it is preferable for technologists to have their work product directly checked by the interpreting physician before the patient leaves the department, in some outpatient settings technologists must make their own decision, and therefore they need to be well trained and using robust and reproducible protocols. The new generation technologists therefore have to be trained in nuclear medicine and CT, to have experience in reviewing scans and to be able to identify artefacts occurring during acquisition

of studies. Instructing the technologists about pertinent history questions and designing a template to be filled out for each patient will ensure that all of the clinical information to further assist in the reading of the images is available. Training requirements for CT and SPECT technologists differ in various countries. Under ideal circumstances a technologist should be fully trained, experienced and certified in both nuclear and X ray/CT technologies.

3. GENERAL NUCLEAR MEDICINE SPECT/CT PROCEDURES

The SPECT component of the SPECT/CT procedure is performed using the acquisition protocols routinely employed for the dual-head gamma camera. This device is equipped with collimators adequate for the specific radioisotope in use, such as low energy, high resolution parallel hole collimators for ^{99m}Tc, or medium energy collimators for ^{67}Ga, ^{111}In or ^{131}I. Imaging is typically performed with the detectors facing each other at 180°, typically acquiring 120 projections over a 360° orbit and using a time per projection of 40–50 s. A 64 × 64 matrix is commonly employed for the low count isotopes, while the higher resolution 128 × 128 matrix can be applied for the higher count rates typically generated by ^{99m}Tc.

CT images are obtained immediately following the SPECT acquisition. For the low-dose CT devices the acquisition parameters include settings at 140 kV, 1–2.5 mA, 13 s/slice, 256 × 256 image matrix, 5 mm slice thickness and slice spacing. For diagnostic CT acquisitions the settings are 140 kV, 80 mA, 1 s/slice, 512 × 512 image matrix, 48 cm reconstruction diameter, 5 mm slice thickness and slice spacing. Skeletal CTs of diagnostic quality can be performed at lower mAs products to reduce the radiation exposure of the patient. A variety of other settings are possible depending on the specific diagnostic question asked of the CT scanner. These include, in particular, protocols to perform low powered CT with the multi-detector scanners, e.g. when a CT of diagnostic quality is already available or high powered CT is not deemed necessary for the particular question under study. Some strategies restrict the CT field of view to the regions exhibiting SPECT abnormalities, thus reducing the radiation dose delivered to the patient even further [6]. Data are reconstructed using filtered back-projection software and filters provided by the manufacturer.

Co-registered CT and SPECT are acquired by translating the patient from one detector to the other while the patient remains lying on the same table. This allows the CT and radionuclide images to be acquired with a consistent scanner geometry and body habitus, and with a minimal delay between the two acquisitions.

3.1. ^{131}I-Iodide SPECT/CT in thyroid cancer

Well differentiated thyroid cancer has an incidence of approximately 1:10 000 [7]. Its standard treatment includes total thyroidectomy and therapy with ^{131}I-iodide [8, 9]. With this combined approach, overall 5 year survival rates exceed 95%. However, the long term prognosis is worse for patients who present with locally advanced tumours or distant metastases at diagnosis, as well as in case of dedifferentiated neoplasms (because of their reduced iodine-trapping property) [10]. This subgroup accounts for approximately 20% of patients with well differentiated thyroid carcinomas and deserves special attention on follow-up.

The therapeutic effect of ^{131}I is provided by its beta-emission. In addition, this isotope of iodine emits 364 keV gamma rays that can be detected by gamma cameras. Therefore, ^{131}I is also used as a diagnostic agent since most, but not all metastases of thyroid carcinoma have

retained the normal thyroid parenchyma's ability to accumulate iodine. The bio-distribution of ^{131}I is usually sufficiently defined by planar scintigraphy. SPECT is only rarely used for this purpose, as the image quality of ^{131}I-SPECT is hampered by the high energy of the gamma radiation emitted by this radionuclide.

^{131}I is only poorly concentrated by most extrathyroidal tissues. The salivary glands, stomach, intestines, and urinary bladder are the most notable exception to this rule. Thus, gamma camera images of ^{131}I distribution in the human body lack anatomical detail, because no clear reference landmarks can be recognized. This renders localization of radioiodine foci difficult, if not impossible at times, and may constitute a problem in those patients in whom surgical removal of metastases is indicated.

Iodine-avid metastases can be small. Furthermore, they may occur in regions exhibiting distorted anatomy due to previous surgery. Their localization using CT or MRI may therefore also not be possible. SPECT/CT co-registration certainly is an elegant method of localization (Fig. 1), although the evidence to this effect is still scarce. Papillary and, albeit to a lesser extent, follicular thyroid carcinomas metastasize frequently to the cervical and mediastinal lymph nodes. Therefore, dissection of the central cervical lymph nodes is, in many cases, part of the initial surgical procedure [11]. Despite a theoretically total thyroidectomy, a variable amount of normal thyroid parenchyma persists within the patient. This provides the rationale for postoperative radioiodine therapy for ablation of thyroid remnants. On the post-therapeutic radioiodine scans, the high activity contained in this parenchymal residue may hamper cervical N staging in many cases. With SPECT/CT, this problem may be overcome (Fig. 2). Preliminary data using SPECT/CT indicate that approximately one fourth of patients may actually harbour cervical lymph node metastases at the time of radioiodine ablation, the majority of which elude detection by planar imaging [12]. Clearly, further longitudinal studies are needed to define the possible clinical impact of this previously unavailable early information on cervical lymph node involvement.

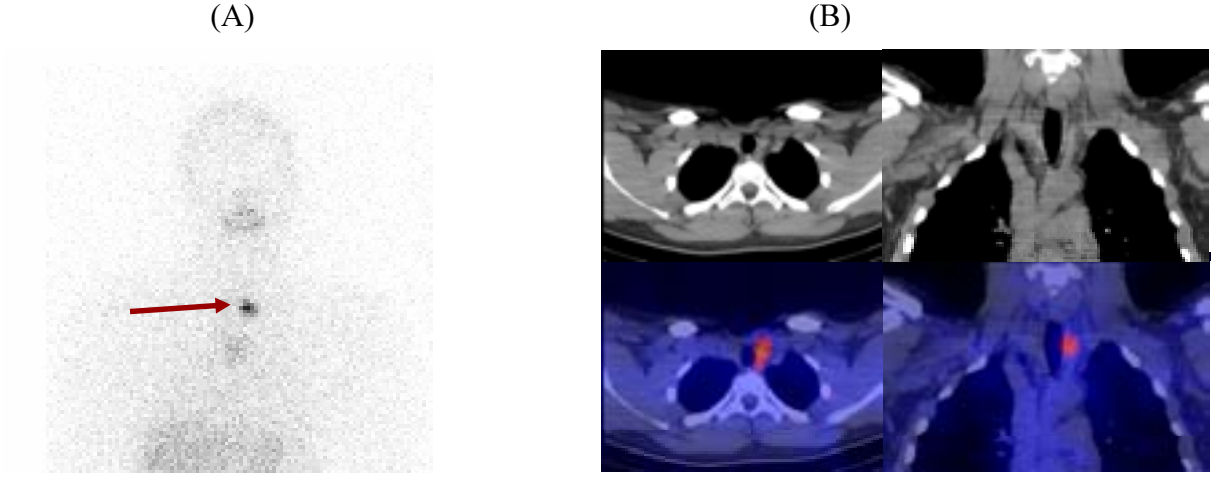

FIG. 1. (A) The planar ^{131}I-iodide scan in a 16 year old patient with thyroid cancer discloses an iodine-avid focus (arrow). The patient had had three surgical procedures (including total thyroidectomy) and 37 GBq of ^{131}I, so that this focus indicates the presence of a further lymph node metastasis. Considering scarring from prior surgeries, exact localization of this lesion is an essential requisite for its surgical resection. This anatomic information can only be achieved by SPECT/CT (B).

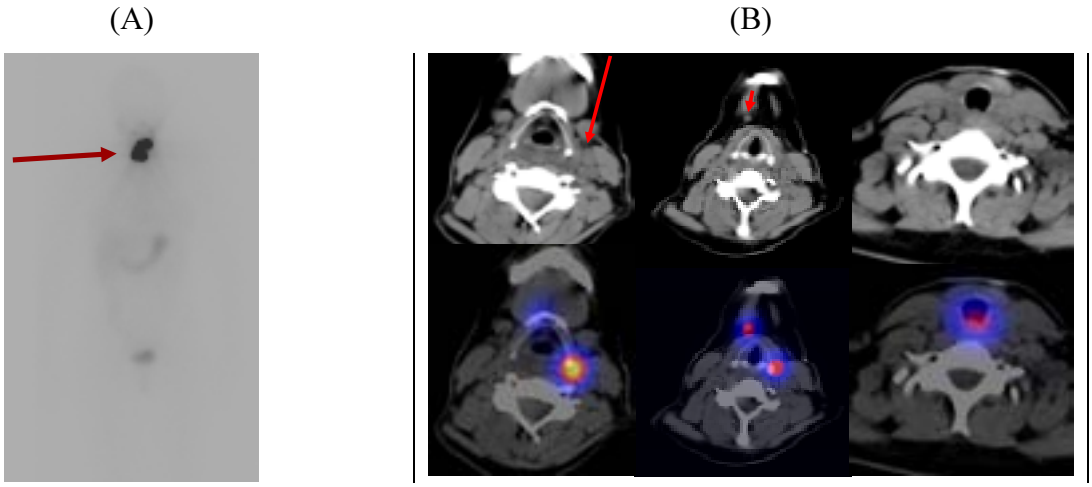

FIG. 2. (A) The planar scan post-radioiodine ablation of thyroid remnants shows radioiodine-avid tissue in the neck of a patient after total thyroidectomy, without the possibility of discriminating ^{131}I uptake in remnant normal thyroid parenchyma from possible lymph node metastasis. (B) SPECT/CT demonstrates two cervical lymph nodes in this patient (arrows) that cannot be differentiated from benign remnant tissue in the planar scan.

Although ^{131}I uptake is quite specific for tissue originating from the thyroid gland, the list of false–positive findings on planar whole body scans is quite long [13]. Only in rare instances, false–positive findings are accounted for by ^{131}I uptake in cancers of non-thyroid origin, such as small-cell bronchial carcinomas. Persisting thymic tissue has been described to concentrate radioiodine and may be the benign correlate of mediastinal ^{131}I accumulation frequently seen in children and young adults. In addition, many false–positive scans are caused by structural abnormalities of organs physiologically excreting radioiodine, or by contaminations of the skin. All such false–positive findings reduce specificity of the scan.

Clearly, ^{131}I uptake in metastases may be mistaken for physiological uptake if it is seen in regions where this usually occurs, thus lowering the sensitivity of ^{131}I scintigraphy. However, probably due to the lack of a reliable gold standard, evidence on sensitivity and specificity of radioiodine scanning is scarce. Furthermore, the recent introduction of ultra-sensitive assays for serum thyroglobulin (a marker of persistent/recurrent disease after surgery and radioiodine ablation of thyroid remnants) is somewhat changing the approach to the follow-up of these patients, especially in the low-risk group [14–18]. Nevertheless, by offering the possibility to precisely localize ^{131}I uptake, SPECT/CT is expected to improve the diagnostic accuracy of radioiodine scanning and therefore to have a significant effect on patient management. As yet two publications have dealt with this issue [12, 19]. Tharp and colleagues retrospectively studied the diagnostic impact of ^{131}I-SPECT/CT imaging in a heterogeneous group of 71 patients with thyroid cancer [12]. In 61 of these, SPECT/CT was used to evaluate the neck, allowing a precise characterization of equivocal lesions on planar imaging in 14/17 patients and changing the assessment of the lesion localization in five patients as compared with planar studies. Thirty-six patients of that group had SPECT/CT for foci of uptake distant from the neck. In this subgroup, SPECT/CT identified equivocal lesions as definitely benign in nine patients. Furthermore, it helped to precisely localize malignant lesions in seventeen patients. The incremental diagnostic value of SPECT/CT was reported to be 57% in the whole group. Ruf et al. investigated the benefit of SPECT/CT hybrid imaging in 25 patients with thyroid carcinoma exhibiting 41 foci of ^{131}I uptake considered inconclusive on planar imaging

[19]. Of these foci, 95% were correctly classified as benign or malignant by hybrid imaging, the gold standard for final classification being represented by clinical follow-up and/or additional ultrasound, CT, or MRI. In the patient based analysis, SPECT/CT was found to change the therapeutic procedure in 25% of the subjects studied.

These pilot studies suggest that diagnostic improvements brought about by SPECT/CT in patients with thyroid carcinoma are considerable. However, considering the variable clinical presentations of differentiated thyroid cancer, validity of the above conclusion should be based on large-scale multi-centre prospective studies enabling stratification of patients into statistically meaningful homogeneous subgroups.

3.2. Neural crest and adrenal tumours

Pheochromocytomas and paragangliomas are chromaffin cell tumours originating from the adrenal medulla and from the paraganglia, respectively. Sympathetic-derived paragangliomas are most frequently located in the retroperitoneum and thorax, while parasympathetic paragangliomas are located near the aortic arch, neck and skull base. These tumours are said to follow in general the 10% rule: approximately 10% are malignant, 10% familial, 10% extra-adrenal, 10% bilateral, and 10% occur in children [20, 21].

Early diagnosis, accurate pre-treatment staging and adequate follow-up are crucial as to the possibility of curing such tumours. Although multi-detector row CT and high-field MRI are reliable for accurate evaluation of these tumours and are usually employed for initial imaging, they are inadequate for whole body assessment (especially MRI).

Radioiodinated metaiodobenzylguanidine (MIBG), an analogue of norepinephrine and guanethidine, was the first radiopharmaceutical capable of specifically depicting and localizing catecholamine-secreting tumours, including pheochromocytomas and paragangliomas. Nowadays, MIBG scintigraphy (generally performed with the ^{123}I labelled radiopharmaceutical) is still regarded as one of the first-choice imaging techniques for diagnosis and follow-up, as it depicts primary and residual or recurrent tumours, as well as metastatic lesions, with an overall accuracy of about 90% [22]. Moreover, in patients with malignant disease, MIBG scintigraphy is an essential step to select patients for ^{131}I-MIBG therapy.

However, the clinical utility of MIBG scintigraphy is often impaired by a lack of accurate anatomical information, in particular with regard to lesion localisation. Nevertheless, the combination of anatomical maps and scintigraphic imaging, as provided by the SPECT/CT hybrid systems, has allowed a significant improvement in localizing MIBG-avid foci (Fig. 3), mainly by more precisely defining the tumoural extension and by increasing specificity (as it permits to exclude disease in foci of tracer uptake identified as sites of physiological accumulation). In this respect, major benefits have been observed in case of tumours located near organs with high physiological tracer uptake, such as liver and myocardium, and when characterizing areas of normal MIBG bio-distribution or excretion, thus avoiding the need for delayed imaging [23, 24].

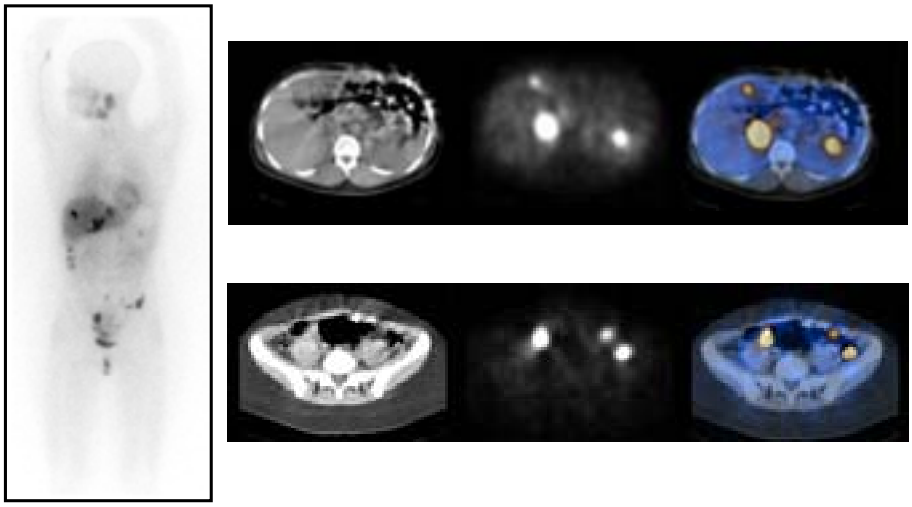

FIG. 3. ^{123}I-MIBG scintigraphy in a 26 year old woman who had undergone laparoscopic left adrenalectomy 5 years earlier because of pheochromocytoma. Despite histological appearance of benign pheochromocytoma, symptoms and biochemical markers of disease recurred, leading to the diagnostic scan. The whole body planar scan (left panel) shows multiple foci of tracer uptake in the abdominal area, most notably in the liver and in other areas suggesting possible lymph node metastases. However, SPECT/CT images (upper and lower right panels) show that such foci represent peritoneal implants rather than visceral or lymph node metastases, possibly secondary to intra-surgical dissemination of benign pheochromocytoma cells.

Ozer et al. have explored the role of fused SPECT/CT imaging for MIBG scintigraphy in a series of 31 patients with suspected pheochromocytoma [25]. In 81% of the cases, fused images correctly characterized the focal tracer uptake detected on planar ^{123}I-MIBG scan as physiological intestinal, renal or hepatic accumulation. Furthermore, SPECT/CT correctly localized focal accumulation in the adrenal glands of four patients and differentiated bone metastases from a local recurrence of pheochromocytoma in two patients. SPECT/CT also discriminated MIBG uptake in a retroperitoneal recurrence from adrenal hyperplasia consequent to contralateral adrenalectomy [26].

Neuroblastomas and ganglioneuroblastomas are poorly differentiated tumours arising from precursors of the sympathetic nervous system that typically occur in infants and young children. Neuroblastoma is the most common extracranial solid tumour of childhood. It may arise anywhere along the sympathetic chain, but most commonly occurs in the adrenal gland, with metastases present in 50–60% of patients at the time of diagnosis. Prognosis is affected by age, site of the primary tumour, and surgical resectability. Ganglioneuroblastomas are transitional tumours of sympathetic cell origin that contain elements of both malignant neuroblastoma and benign ganglioneuroma [21]. The most common tumour sites are the adrenal medulla (35%), retroperitoneum (30–35%), posterior mediastinum (20%), neck (1–5%), and pelvis (2–3%).

MIBG scintigraphy is useful not only for identifying the primary tumours, but also to monitor the pattern of metastatic spread (with an overall 92% sensitivity and 96% specificity) and response to treatment [22]. However, fused SPECT/CT images are expected to further improve its diagnostic accuracy, especially if performed in selected cases, i.e. in patients with inconclusive planar or SPECT imaging with respect to the exact anatomic localization of the lesions detected on the scintigraphy. In particular, given the relatively high frequency of

skeletal metastases in neuroblastomas, SPECT/CT can differentiate between bone and bone marrow involvement. Moreover, hybrid imaging helps to characterize tumour recurrence in close vicinity to the heart or liver, organs with high physiological MIBG uptake. On the other hand, in paediatric patients SPECT/CT may help to clarify the diffuse physiologic tracer uptake in the right heart sometimes misinterpreted as malignant mediastinal, sternal or vertebral sites of tumour involvement [23, 26].

SPECT/CT provides therefore a clinically useful option for localizing sites of abnormal MIBG uptake and for characterizing their benign or malignant nature. In addition to increasing specificity of staging and providing useful anatomic information on surgical resectability, the procedure also has an impact on the selection of patients to be treated with ^{131}I-MIBG.

3.3. ^{111}In-octreotide SPECT/CT for assessing neuroendocrine tumours

^{111}In-octreotide scintigraphy is widely employed to image somatostatin–receptor-positive neuroendocrine tumours. Over the last decades, lesion detection and overall clinical accuracy have improved due to optimized imaging techniques. The currently injected dose of 6 mCi of ^{111}In-octreotide (^{111}In-DTPA-pentetreotide) has doubled as compared to the 3 mCi dose administered in the initial studies. SPECT imaging is now routinely performed.

Neuroendocrine (NE) tumours of the gastrointestinal tract include carcinoid and islet-cell tumours, and surgery is the treatment of choice. Detection of all tumour sites is critical for referring patients to surgery and for its optimal planning. Localization of lesions may be difficult, due to their small diameter and lack of anatomical delineation [27]. The sensitivity of conventional imaging modalities, mainly CT and ultrasound, ranges between 13% and 85%, depending on the type, site and size of the tumour and on the imaging protocol [28].

Many neuroendocrine tumours show an increased expression of somatostatin receptors. A variety of analogues with high binding affinity to somatostatin receptors have been synthesized. One of these is octreotide, an eight amino acid cyclic peptide, with a biologic half-life measured in hours, which is used as an injectable therapeutic agent to inhibit excess secretions from neuroendocrine tumours. Somatostatin receptor scintigraphy is based on the use of octreotide as a carrier of radionuclides for diagnostic imaging or targeting therapy. A tyrosyl moiety in position 3 of the cyclic amino acid ring, the tyrosyl^3-octreotide has been substituted initially with ^{123}I [29]. Since ^{123}I is an expensive and short lived radioisotope, the use of ^{111}In bound to the octreotide molecule, ^{111}In-DTPA-pentetreotide, has been further developed, with the original octreotide eight amino acid molecule covalently bound to DTPA that, in turn, serves to link the radiometal [30].

Diagnosis, staging and follow-up of neuroendocrine tumours have advanced considerably with the advent of ^{111}In labelled pentetreotide scintigraphy. This modality has a reported sensitivity of 82–95%, and can successfully detect previously unknown sites of disease, undetected by conventional imaging techniques, in 30–50% of various NE tumours [31, 32]. Octreotide scintigraphy improves the localization and staging of primary tumours and enables early detection of recurrence [33]. In addition, octreotide scintigraphy facilitates the detection of receptor-dense microscopic foci during radio-guided surgery and is being used to determine if the whole tumour has been resected. Scintigraphy is also being used to define the receptor-status of metastases for octreotide treatment [34–36] or for targeted receptor-mediated radiotherapy [37–39]. It has been previously demonstrated that octreotide scintigraphy induced a change in classification in 24% and in surgical strategy in 25% of

patients with gastro-entero-pancreatic tumours [40], and changed the patient management in 47% of patients with gastrinomas [41].

Despite the valuable contribution of planar and/or SPECT ^{111}In-octreotide scintigraphy to the diagnosis and management of patients with known or suspected neuroendocrine tumours or other processes characterized by the increased expression of somatostatin receptors, the patterns of distribution of ^{111}In-octreotide have raised the need for correlating scintigraphic findings with anatomic imaging results. The overall specificity of scintigraphy may be affected by tracer uptake in physiological sites or in benign conditions. False–positive interpretations may be caused by the high receptor status of normal organs, such as the pituitary gland, thyroid, liver and spleen, or by physiological excretion of the tracer via the kidneys or the bowel. Hepatobiliary excretion, accounting for clearance of 2% of the administered dose, may lead to occasional visualization of the gallbladder which may potentially be misinterpreted as hepatic metastasis [42]. Guidelines for octreotide scintigraphy therefore recommend performing delayed studies that demonstrate changes in tracer kinetics and thus provide the differential diagnosis between benign, physiologic and malignant sites of radiotracer uptake. Neuroendocrine tumours are often localized in the abdomen and it can be difficult to precisely localize a suspicious lesion, or to differentiate whether a focus of abnormal uptake is in the pancreas, small bowel, liver or bone without anatomic correlation. In the region of the liver, it is difficult to distinguish between physiologic gallbladder accumulation versus a lesion in the head of the pancreas, in the right adrenal or in the small bowel.

Octreotide scintigraphy, although highly sensitive, is limited by the lack of precise anatomic localization, and requires correlation with high resolution anatomic imaging modalities in a large number of cases [40, 43]. Side by side interpretation of the two image sets (SPECT and CT) acquired separately, as well as co-registration of separately acquired anatomic (usually CT) and SPECT ^{111}In-octreotide imaging data have been developed. These techniques work quite well for fusion of studies of the brain, as there is no shift of the intra-cranial content from one study to another. In the thorax, there are differences in organ and lesion position depending on respiratory dynamics. Central mediastinal structures have limited excursion so that satisfactory co-registration, although very cumbersome and time-consuming, can be achieved. In the abdomen and the pelvis, there is the potential for significant shift of lesions depending upon patient positioning and variations in stomach, bowel or bladder distension. This represents a challenge for co-registration of separately performed SPECT and CT examinations, even when they are obtained within a close temporal interval, leading to possible mis-alignment of suspicious foci. A software package has been used to fuse helical CT and SPECT images of 28 lesions identified in 10 patients, using either external fiducial markers or internal anatomic landmarks (spleen and kidney contour) [44], and a shift of a few mm in organ location between SPECT and CT has been demonstrated. The use of image co-registration in the preoperative staging of patients with gastro-entero-pancreatic neuroendocrine tumours following ^{111}In-octreotide administration has also been evaluated in 38 patients with 87 lesions [45]. The accuracy of successfully assigning the anatomical location by two independent readers increased from 57% and 61% to 91% and 93%, respectively, using co-registration. Diagnosis and localization of liver metastases to a specific segment improved from 45% and 58% to 98% and 100%, respectively, with relevant information for further therapeutic decisions in 19% of the patients [45]. Nevertheless, the approach of co-registering separately performed octreotide-SPECT and CT studies cannot be considered as the optimal approach for assessment of function and anatomy of neuroendocrine tumours.

SPECT/CT may localize foci of increased tracer activity to normal organs with known physiological activity, without the need for performing delayed scans on additional days. SPECT/CT may also improve image interpretation when the foci of increased tracer uptake can be precisely localized to octreotide-avid benign processes, such as recent surgery or colostomy, increased thyroid uptake in Graves' disease, accessory spleen, parapelvic cyst, benign breast lesions and granulomatous lung disease (e.g. sarcoidosis) [34, 46]. When active malignant disease is diagnosed, SPECT/CT can precisely define the organ involved and determine the presence or absence of invasion into surrounding tissues. Following the diagnosis and localization of neuroendocrine tumours, SPECT/CT may also help in determining the extent of disease, defining it as localized or disseminated, and thus influence the choice of the most appropriate treatment modality [47–49]. When disease is confined to a single organ, a localized mode of organ-specific therapy is suggested, such as surgery or chemoembolization (Figs 4, 5). When a soft-tissue tumour has invaded the adjacent bone, surgery is inadvisable. In extensive, unresectable disease, systemic therapy is required.

Initial studies have shown that SPECT/CT had an impact on patient management in 5 out of 10 patients with neuroendocrine tumours [50]. Further studies have indicated that octreotide SPECT/CT has a specificity of 86% and a positive predictive value of 85% for diagnosis of neuroendocrine tumours, and resulted in a change in management in 3–14% of patients [46, 49]. Pfannenberg et al., in an analysis of 43 patients with neuroendocrine tumours, compared SPECT/CT results to those of SPECT and to high-end CT stand-alone images, histopathology or clinical and imaging follow-up representing the diagnostic standard. Separate SPECT and CT interpretations were in agreement for 56 of 114 lesions overall (49% concordance). For the remaining 58 lesions (51%), consensus readings of the fused SPECT/CT images resulted in a change from the original interpretation of 39 CT and 19 SPECT examinations. Overall, SPECT/CT outperformed significantly both SPECT and high-end CT. The greatest accuracy involved the use of SPECT/CT with side by side availability of high-end CT. In fact, in this report SPECT and side by side high-end CT performed slightly better than SPECT/CT [51]. A preliminary report of ^{111}In-octreotide SPECT/CT in 27 patients with suspected or known neuroendocrine tumours, primarily of the gastro-entero-pancreatic type, indicated that fused images improved the overall diagnostic confidence in 15 of 27 cases [52].

In a large series including 72 patients with neuroendocrine tumours, Krausz et al. evaluated the impact of SPECT/CT on the diagnostic accuracy of octreotide scintigraphy and on further clinical patient management [47]. SPECT/CT improved the study interpretation in 32% of the total study population (52% of the positive studies). SPECT/CT allowed for the precise localization of foci of increased ^{111}In-octreotide activity thereby defining the whole extent of disease in 17 patients, it diagnosed previously unsuspected bone metastases in 3 patients and defined suspicious lesions as sites of physiologic activity, unrelated to cancer, in 3 additional patients. SPECT/CT altered the subsequent management of 10 patients (14%). Results of fused images modified the previously planned surgical approach in 6 patients, spared unnecessary surgery in 2 patients with newly diagnosed involvement of the skeleton, and led to referral of one patient each to liver transplant and to chemoembolization, rather than to systemic therapy.

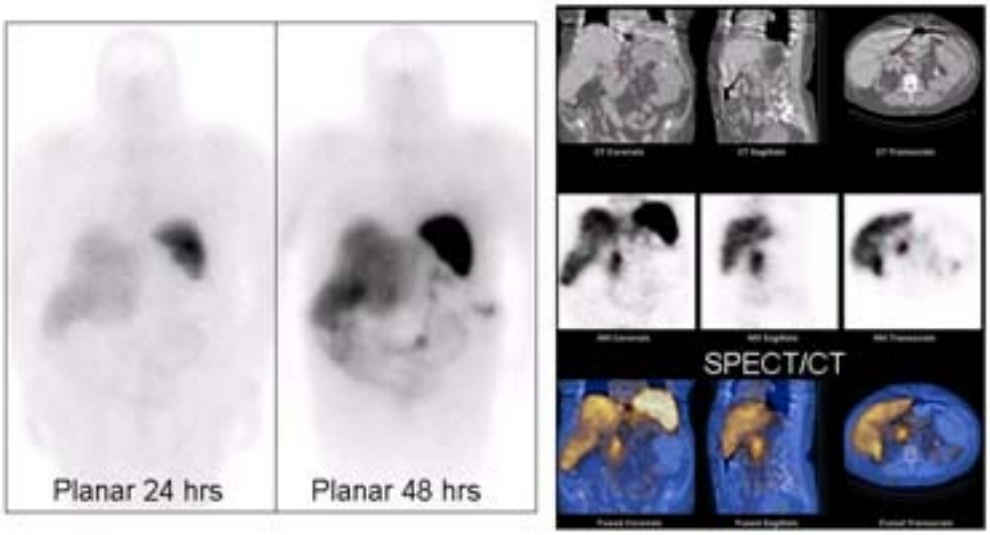

FIG. 4. ^{111}In-octreotide SPECT/CT in duodenal carcinoid. A 56 year old woman with duodenal carcinoid diagnosed following biopsy of a duodenal ulcer was referred for defining extent of disease prior to treatment planning. Whole body planar scans performed at 24 and 48 h after tracer injection are normal. SPECT demonstrates a small focus of abnormal tracer activity in the right mid-abdomen, localized by SPECT/CT fused images to the duodenum, consistent with the known primary tumour. No additional sites of abnormal tracer activity are seen. The patient was referred for surgery.

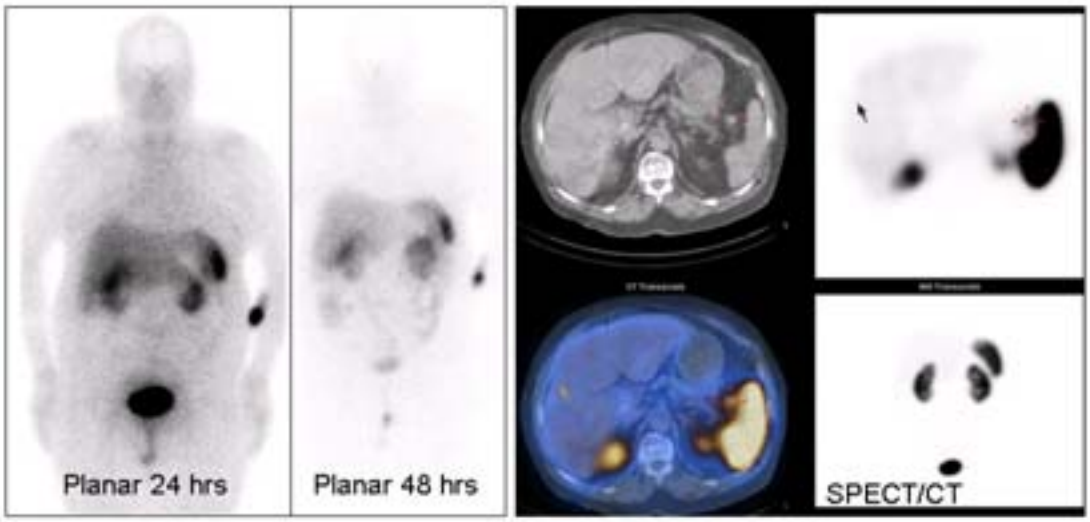

FIG. 5. ^{111}In-octreotide SPECT/CT in pancreatic insulinoma. A 68 year old woman was hospitalized because of severe hypoglycemia. CT indicated a suspicious lesion in the tail of the pancreas. Whole body planar scans performed at 24 and 48 h after tracer injection are normal. SPECT demonstrates a small focus of abnormal tracer activity in the left upper abdomen, in close proximity to the high ^{111}In-octreotide uptake in the spleen. This suspicious lesion is localized by SPECT/CT fused images to the small lesion seen on CT in the tail of the pancreas, consistent with a pancreatic insulinoma. No additional sites of abnormal tracer activity are seen. The patient was referred for surgery.

Octreotide-SPECT/CT provides information regarding the functional status of the tumour, its precise localization and the whole extent of disease. Fused images are therefore useful tools to choose the optimal treatment strategy, mainly in patients with advanced disease. When scintigraphy is negative, SPECT/CT is of no additional value except for verification of receptor density in a tumour visualized on CT. SPECT/CT provides greater accuracy in localization of findings than functional SPECT imaging alone and greater specificity than anatomic CT as a stand-alone procedure.

In summary, despite the favourable impact that ^{111}In-octreotide scintigraphy, particularly SPECT, has had on the diagnosis and management of patients with neuroendocrine tumours, these features improve even further when correlated with anatomic imaging data acquired sequentially during a single imaging session. Criteria for improvement include higher diagnostic sensitivity and specificity, as well as impact on patient management. Thus, it can be concluded that near simultaneous acquisition of both CT and SPECT image sets (hybrid SPECT/CT) represents the state of the art for diagnostic ^{111}In-octreotide imaging of neuroendocrine tumours.

3.4. ^{67}Ga-citrate SPECT/CT in lymphoma

^{67}Ga-citrate scintigraphy has long been shown to be useful for evaluating patients with lymphoma, and SPECT/CT has further improved its diagnostic sensitivity as well as localization of areas with abnormal tracer uptake [53]. In particular, SPECT/CT proved to be very helpful for distinguishing spinal lesions from adjacent nodal involvement. It was also able to clarify the tracer uptake at the edges of the lower chest, projecting over the hepatic dome, ribs or sternum. Furthermore, SPECT/CT imaging has been shown to provide additional information or diagnosis from CT-detected abnormalities leading to significant change in patient's management [54].

3.5. Lymphoscintigraphy

Accurate lymph node staging is essential for the treatment and prognosis in patients with cancer. The sentinel lymph node is the first node to which lymphatic drainage and metastasis from the primary tumour occur. Procedures for sentinel lymph node detection and biopsy have already been implemented into clinical practice [55, 56]. Precise anatomic localization of the sentinel lymph node is critical for minimally invasive surgery and to avoid incomplete removal of the sentinel node, especially in the regions of the head and neck, the chest and the pelvis.

In the head and neck the lymphatic drainage is in the levels I through VII. A node in level I-A is in the subdigastric muscle area, and a node in level I-B is in the submandibular area. A node in level II-A is anterior to the sternocleidomastoid (SCM) muscle, and a node in level II-B is adjacent to the SCM muscle. Nodes in level II are above the hyoid bone. A node in level III is adjacent to the SCM muscle, between the hyoid bone and the cricoid cartilage. A node in level IV is adjacent to the SCM muscle below the cricoid cartilage. A node in level V-A is behind the SCM muscle above the cricoid cartilage, and a node in level V-B is behind the SCM muscle below the cricoid cartilage. A node in level VI is in the anterior middle neck between bilateral SCM muscles, and a node in level VII is in the superior mediastinum.

Axillary lymph node levels are level I (low) lateral to the pectoralis minor (PM) muscle, level II (mid) behind the PM muscle, and level III (high) medial to the PM muscle.

The resection of external iliac *versus* inguinal lymph nodes requires significantly different surgical approaches, and thus precise preoperative localization is crucial for optimal surgical approach. A node above the level of the inferior epigastric artery which is anterior and lateral to the bladder base is an external iliac node, and the nodes below the inferior epigastric artery are inguinal nodes, further subdivided into superficial and deep ones by the sapheno-femoral venous junction.

Only SPECT/CT imaging can precisely locate the sentinel lymph node since CT images provide critical anatomical landmarks such as the hyoid bone, cricoid cartilage, SCM and PM muscles, inferior epigastric artery and sapheno-femoral venous junction.

SPECT/CT increases the sensitivity and specificity of lymphoscintigraphy, and also provides the additional diagnostic information from the CT images [57–62]. A standard dose of 0.5 mCi ^{99m}Tc labelled colloid (5–80 nm) is injected intradermally around the melanoma lesion, interstitially around the breast cancer lesion and subcutaneously around other tumours. SPECT/CT is usually obtained immediately after identifying drainage of the activity on serial planar images (Fig. 6).

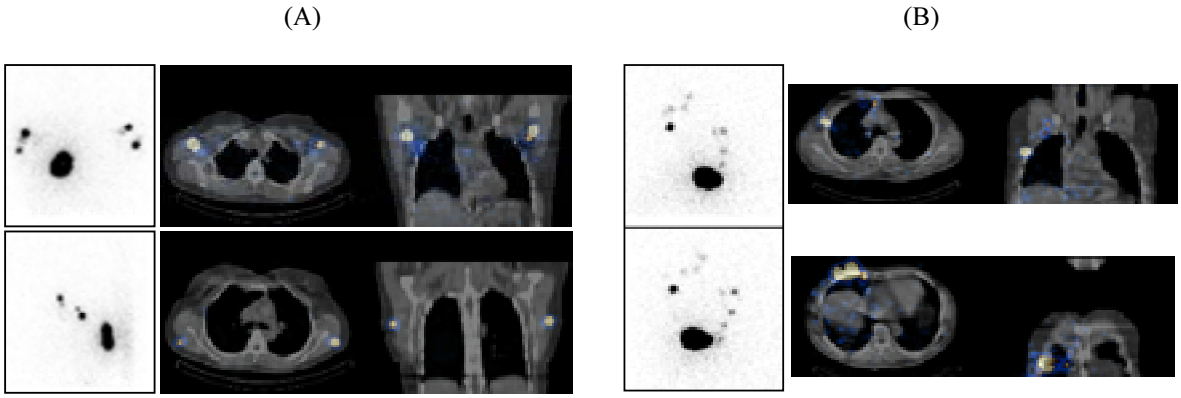

FIG. 6. Additional information over planar scintigraphy provided by SPECT/CT in two patients with malignant cutaneous melanoma submitted to lymphoscintigraphy with ^{99m}Tc-albumin nanocolloid before radioguided sentinel lymph node biopsy. (A) Left panels show the planar posterior (top) and left lateral (bottom) views in a patient with melanoma located on her back: multiple bilateral lymph nodes can be detected, without however clear reference to precise anatomic structures. Right panels show SPECT/CT tomographic sections at different levels, demonstrating bilateral lymphatic draining to both axillary (top) and subscapular (bottom) lymph nodes. (B) Left panels show the planar right oblique (top) and anterior (bottom) views in a patient with melanoma located on his anterior right chest: multiple lymph nodes can be detected, without however clear reference to precise anatomic structures. Right panels show SPECT/CT tomographic sections at different levels, demonstrating lymphatic draining to both axillary and internal mammary chain lymph nodes

3.6. Skeletal scintigraphy for staging malignant disease

Scintigraphic imaging of bone metabolism is a cost efficient way to prove or exclude skeletal metastases in patients with tumours prone to metastasize to the skeleton, such as breast, prostate, or lung carcinomas [63]. Therefore, bone scintigraphy is included in the majority of guidelines addressing management of these neoplastic conditions in many countries and is one of the most frequently performed radionuclide imaging procedures performed worldwide.

In a recent study comparing the diagnostic accuracy of ^{99m}Tc-phosphonate skeletal scintigraphy to that of [^{18}F]FDG-PET in patients with thyroid carcinoma [64], sensitivity of the conventional procedure was not significantly different from that of [^{18}F]FDG-PET. However, its specificity was significantly worse. This result can be considered representative also of other tumours and is not at all unexpected, since there are several highly prevalent benign conditions leading to focally increased uptake of the radiolabelled phosphonates in the skeleton. Most of these conditions reflect degenerative processes of the joints increasing in frequency with age, such as spondylarthrosis or coxarthrosis. Additional benign causes of enhanced uptake are rheumatic disease or benign bone tumours.

Since most of these benign conditions are readily identifiable on CT, SPECT/CT is expected to improve specificity of skeletal scintigraphy without reducing its sensitivity. Besides single case reports illustrating this assumption, several prospective studies have investigated this issue.

In 2004, Horger et al. demonstrated significantly increased specificity when using SPECT/low-dose non-spiral-CT for classifying 104 lesions in 47 subjects exhibiting indeterminate findings on conventional planar imaging [65]. This study is particularly valuable considering that the reference gold standard for final classification of lesions was either histological confirmation or extended clinical follow-up, and thus independent from the results obtained by SPECT/CT.

Römer et al. employed a SPECT/CT camera equipped with a two slice spiral-CT for classifying 52 lesions in 44 patients, defined as indeterminate on SPECT imaging [6]. These authors reported that SPECT/CT enabled correct classification of the scintigraphic abnormalities in 92% of the subjects studied.

Utsunomiya et al. used a hardware set-up comparable to that of a hybrid SPECT/CT camera, by transferring the patient positioned on the same table in an identical position from a stand-alone SPECT camera to a gantry of an 8 slice CT [66]. By studying 45 patients and based on receiver-operation curve (ROC) analysis, they confirmed the significant increase in diagnostic accuracy brought about by co-registration of these two modalities. Furthermore, they also showed that co-registration performs significantly better than side by side viewing of the two sets of images (SPECT and CT, respectively) on the same workstation.

Considering the evidence summarized above, one cannot but conclude that skeletal SPECT/CT is the new imaging gold standard when searching for osseous metastases and that for this purpose conventional scintigraphy becomes obsolete (Fig. 7). Unsettled issues include the quality of the CT integrated into the hybrid system needed for this purpose, as well as the relative diagnostic accuracy of this approach compared to whole body MRI and PET using [^{18}F]FDG or ^{18}F-fluoride. Although these options appear attractive, a cost effectiveness analysis might strengthen the role of SPECT/CT in this context.

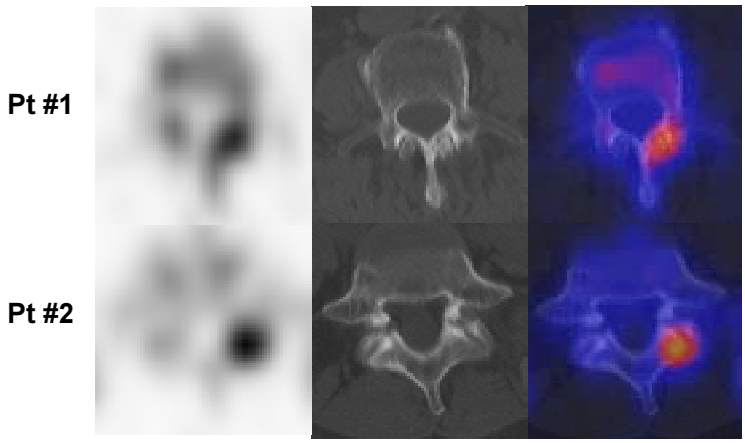

FIG. 7. The upper row shows SPECT, CT, and fused images of a lumbar vertebra in a patient with breast cancer (Pt #1). In this patient, increased uptake of ^{99m}Tc-MDP is due to arthrosis of the facet joint. The lower row depicts similar images in another breast cancer patient (Pt #2). Although the SPECT appearance of the lesion is quite similar to that in Pt #1, the CT overlay proves it to be a small osteolysis.

3.7. Skeletal SPECT/CT in orthopaedics

Up until approximately 20 years ago, planar X ray and skeletal scintigraphy were the imaging procedures of choice in patients with benign orthopaedic disease. Although MRI has brought a dramatic change to the predominance of radionuclide imaging in this field, skeletal scintigraphy still holds the promise of sensitively depicting functional alterations of bone. However, difficulties in precisely localizing abnormalities of bone metabolism relative to the complex anatomy of the skeleton have greatly weakened its clinical role, despite its much lower costs than MRI.

In principle, SPECT/CT would be suited to overcome these problems as demonstrated in several case reports (Fig. 8) [67]. However, so far only one study has systematically studied the clinical benefit of SPECT/CT in orthopaedic disease [68]. Using a SPECT/multi-slice non-spiral CT, Even-Sapir et al. analysed skeletal image data from 89 consecutively studied, non-oncological patients. These patients had non-specific lesions on planar skeletal scintigraphy for which correlation with morphological imaging was considered necessary. The indications for radionuclide bone imaging were pain in 61, prior trauma in 7, suspected infection or inflammation in 6, and fever of unknown origin in the remaining 2 patients. Gold standard for final classification was consensus opinion among the readers, and this represents a possible limitation of the study since it was not independent from SPECT/CT itself. Hybrid imaging enabled a definite diagnosis to be reached in 59% of the patients studied, obviating the need to perform additional imaging. In another 30% of patients, SPECT/CT provided information relevant for their further diagnostic workup. The authors therefore concluded that SPECT/CT is a clinically relevant component of the diagnostic process in patients with non-oncological disease referred for bone scintigraphy.

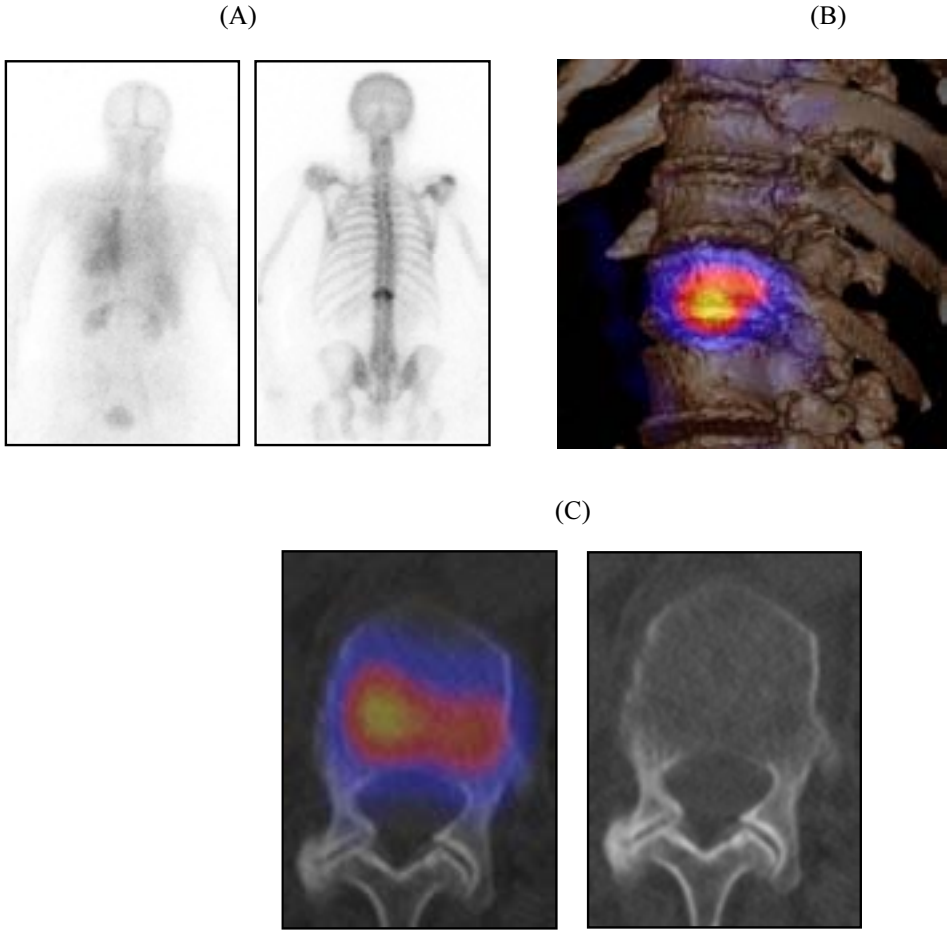

FIG. 8. (A) Early (left panel) and late (right panel) posterior planar skeletal scintigrams of a 74 year old patient after recent trauma, showing enhanced uptake of ^{99m}Tc-MDP in a vertebral body of the lower thoracic spine. 3-D-volume rendering of the SPECT/CT fusion (B) shows that the lesion is in the twelfth vertebral body. The inspection of the fused tomograms (C) proves it to be a fracture; moreover, the one-stop shop examination discloses it to be unstable since the posterior corticalis is involved, thus motivating immediate surgery.

3.8. ^{201}Tl-chloride in cerebral masses

The diagnosis of a postoperative residual brain tumour is a challenging clinical problem, since both contrast-enhanced CT and T1-weighted MRI after surgery are difficult to interpret while precise diagnosis is needed for planning radiation therapy. Likewise, in HIV infected patients, the differential diagnosis between primary lymphoma and cerebral toxoplasmosis is often problematic.

Thallium is a metallic monovalent cationic element in group III-A of the periodic table of elements. ^{201}Tl is cyclotron-generated and is administered in the form of thallous chloride. The cellular uptake of ^{201}Tl after i.v. administration depends on both blood flow and the cellular extraction fraction, which mainly occurs via the Na^+/K^+-ATPase active transport membrane pump in viable cells. A minor fraction of ^{201}Tl uptake is also related to co-transport system, calcium ion channel system, vascular immaturity with ‘leakage’, and increased cell membrane permeability. Tumour cells have shown greater ^{201}Tl uptake than normal

connective tissue or inflammatory cells. In primary brain tumours alterations in the blood-brain barrier play a key role in ^{201}Tl accumulation [69].

In normal subjects little ^{201}Tl activity is seen in the cerebral substance, since ^{201}Tl cannot pass the blood-brain barrier and diffuse into the brain tissue. Conversely, high radioactivity is seen in the orbits, the base of the skull and nasopharyngeal region, and around the scalp. There are no significant differences between early (10 minutes) and delayed (3 hours) images. In case of brain haematoma, ^{201}Tl uptake seen in early images significantly decreases on delayed scans [70].

Postoperative ^{201}Tl SPECT demonstrated a significantly better accuracy than contrast-enhanced CT in detecting residual tumour in 33 patients [71]. Actually, disruption of the blood-brain barrier during the postoperative period often leads to uncertainty in CT interpretation. Co-registration and fusion of ^{201}Tl SPECT with CT could thus optimize postoperative radiation therapy planning through a truly anatomo-metabolic image.

^{201}Tl SPECT has also been seen to be useful for differentiating brain tumour recurrence from radiation necrosis or gliosis after radiotherapy, with more reliable information than CT and MRI in identifying progression, improvement or no change in brain tumours in follow-up studies [72, 73].

Because ^{201}Tl does not accumulate in normal brain parenchyma, anatomical localization of increased tracer uptake is difficult. Registration and fusion with anatomical images facilitates this task during the clinical workup of patients with brain tumours [74]. Appropriate attenuation correction based on the CT transmission data could also help in the reconstruction of ^{201}Tl SPECT images, which will further improve image contrast and detectability of areas of increased uptake, leading to a higher sensitivity of ^{201}Tl imaging, particularly for infratentorial and small size tumours. Until now, physicians have relied mainly on their spatial sense to mentally reorient and overlap ^{201}Tl images with the anatomic data. This approach is inconsistent and highly subjective and can yield suboptimal results because it does not take full advantage of all the available information [74]. Image fusion allows accurate determination of the anatomic sites of normal and abnormal uptake (Fig. 9). The precise localization of ^{201}Tl accumulation is essential to guide the choice of biopsy site (conventional or stereotactic), in an effort to decrease the potential for tissue sampling error in the pathologic specimen, or for planning radiosurgery [75]. Moreover, the accurate assessment of ^{201}Tl uptake can be of significant value after surgical and/or radiotherapy treatment in planning further therapeutic strategies, such as additional surgery or radiotherapy, because CT and MRI are often unable to distinguish residual tumour from post-therapy changes. Fused images can also help in optimizing the treatment specifically to the viable malignant tissue and in the early diagnosis of recurrence during follow-up.

3.9. ^{99m}Tc-depreotide in solitary pulmonary nodules

The characterization of solitary pulmonary nodules (SPNs) represents an important clinical problem because, although they may be caused by many benign conditions, bronchogenic carcinoma is being increasingly identified as one of the main etiologies, especially in the elderly. Survival rate at 5 years may be ≥80% in patients with resected malignant SPN, while it is <5% for patients with advanced malignant disease. Ideally, diagnostic approaches to SPN would permit definitive resection when possible and avoid resection in patients with benign disease [76].

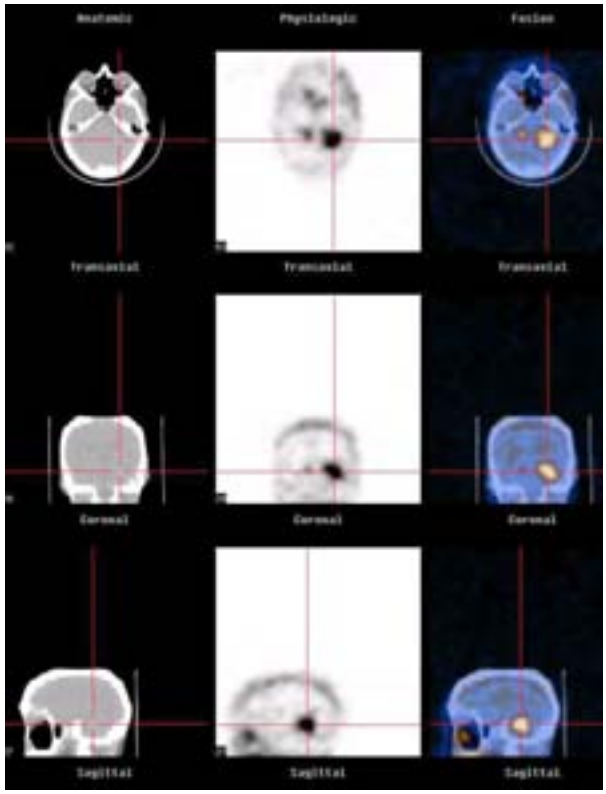

FIG. 9. SPECT/CT performed after administration of ^{201}Tl-chloride in an HIV infected patient referred for differential diagnosis between primary lymphoma and cerebral toxoplasmosis. ^{201}Tl accumulation in the left hemi-cerebellum supports the diagnosis of primary lymphoma.

Depreotide is a synthetic cyclic peptide, an analog of somatostatin, that binds with high affinity to somatostatin receptors 2, 3, and 5. Radiolabelled with ^{99m}Tc, this agent has successfully been used for SPN imaging [77]. In fact, ^{99m}Tc-depreotide has been approved by the US Food and Drug Administration for the noninvasive differentiation of SPN, and it represents a cost effective alternative to [^{18}F]FDG-PET in this application [78]. ^{99m}Tc-depreotide SPECT and [^{18}F]FDG-PET have demonstrated the same specificity (86%) for small (up to 1.5 cm), and equal sensitivity (92%) for large (more than 1.5 cm) SPNs [79]. The role of ^{99m}Tc-depreotide in staging patients with non-small cell lung cancer is still under investigation, although an elevated number of false–positive results have been reported in the hilar/mediastinal regions due to nonspecific tracer uptake [80, 81]. SPECT/CT may help image interpretation by improving specificity at diagnosis and staging and by differentiating physiologic activity (parahilar mediastinal region, bone marrow uptake in the spine, ribs and sternum) from malignant uptake in the primary tumour or into metastatic lymph nodes (Fig. 10). Additionally, the improvement in image quality by the use of X ray based attenuation-correction could increase the detection rate of smaller nodules.

3.10. ProstaScintigraphy

Functional or molecular imaging of prostate cancer presents a challenging problem because of the deep anatomical location of the prostate gland in the pelvis, which causes significant attenuation and scattering problems. Patient's movement, changes of the prostate volume, as well as changes in the shapes and contents of the rectum or bladder during imaging can further exacerbate the problem in image-fusion multimodality imaging visualization of the prostate.

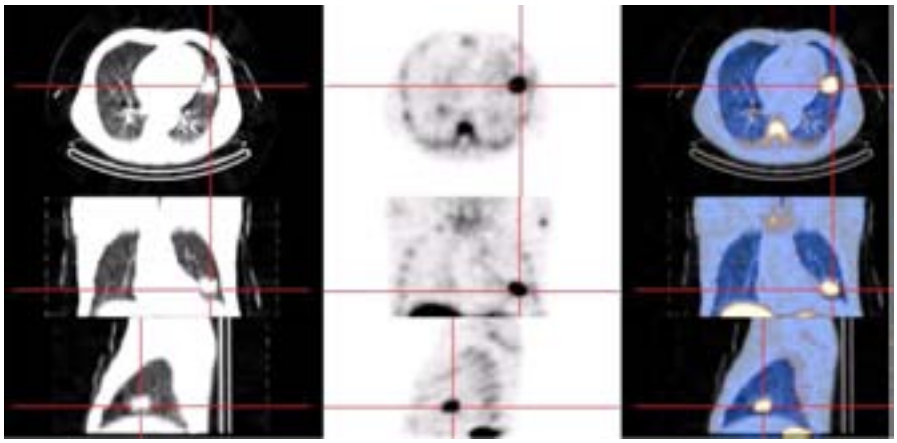

FIG. 10. Transaxial, coronal, and sagittal tomograms of SPECT/CT imaging obtained after injection of ^{99m}Tc-depreotide in a patient with a solitary pulmonary mass occasionally discovered on chest X ray. Intense tracer uptake indicates malignancy, while the fused SPECT/CT images suggest that, while there is no extension of the tumour to infiltrate the chest wall, there is possible involvement of the pericardium.

The overall diagnostic accuracy of imaging using 5 mCi ^{111}In-ProstaScint (monoclonal antibody against the prostate-specific membrane antigen) has been reported to be 76%, with 44% sensitivity and 86% specificity relative to histologic findings [82, 83]. Increased accuracy of the ProstaScint scan for diagnosis of prostate cancer has been reported when fusing SPECT images with either CT or MRI [84, 85]. In addition, ProstaScint imaging can be applied to guide brachytherapy or intensity-modulated external-beam radiation therapy [86], as well as radioimmunotherapy using ^{90}Y-capromab pendetide for recurrent prostate cancer [87].

3.11. SPECT/CT in the preoperative localization of parathyroid adenomas

Parathyroid scintigraphy with ^{99m}Tc-sestamibi (employed either as a single-tracer, dual-phase protocol or in combination with other tracers with exclusive uptake in the thyroid for subtraction imaging) is critical for preoperative localization of parathyroid adenomas, especially in the perspective of applying mini-invasive parathyroid surgery [88–90]. Even before the introduction of hybrid SPECT/CT instrumentation into clinical routine, stand-alone SPECT procedures had already demonstrated clear superiority to planar ^{99m}Tc-sestamibi scintigraphy for imaging and localizing parathyroid adenomas, especially when planning the best surgical approach to ectopic adenomas, mainly located in the mediastinum [91–98].

However, because of the paucity of anatomic landmarks in pure SPECT images, some form of multimodality co-registration often turned out to be useful for better localization of adenomas relative to critical anatomic structures, such as those available through side by side viewing with, e.g. CT images or by post-acquisition image fusion. Useful complementary information as to location of ectopic parathyroid adenomas can also be derived by sequential acquisition, after ^{99m}Tc-sestamibi scintigraphy, of scintigraphic images obtained by injecting a second tracer, e.g. an intravascular indicator such as radiolabelled albumin or red blood cells, to identify the topographic relationships of adenomas with the principal vascular structures [88].

The recent growing-scale implementation of hybrid SPECT/CT equipments has dramatically improved this scenario, by enabling simultaneous acquisition and accurate single hardware

co-registration of functional images (derived from ^{99m}Tc-sestamibi scintigraphy) and of the corresponding morphologic images (derived from CT). Thus, it can be concluded that, at present, SPECT/CT represents the state of the art in preoperative localization of parathyroid adenomas, especially in cases of ectopic location and in the presence of concomitant multinodular goiter (Fig. 11). In all these conditions the localizing performance of SPECT/CT is clearly superior to both planar scintigraphy and stand-alone SPECT.

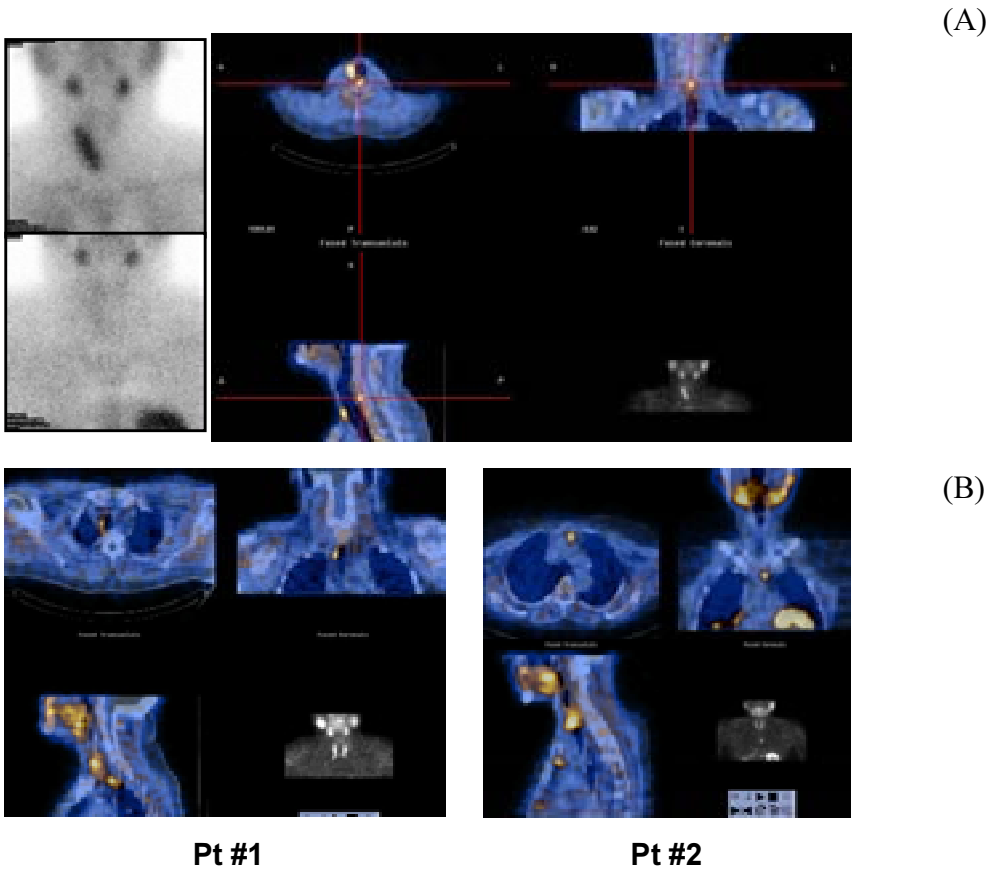

FIG. 11. Patients with parathyroid adenomas in whom hybrid SPECT/CT imaging turned out to be crucial for accurate preoperative localization and for planning the most adequate surgical approach. (A) Early (top left) and delayed (bottom left) planar ^{99m}Tc-sestamibi scans in a patient who had undergone unsuccessful parathyroid surgery during which the left thyroid lobe was also resected because of concomitant nodular goiter (persistent primary hyperparathyroidism despite removal of an enlarged parathyroid gland ectopically located in the anterior mediastinum that had been identified on a planar ^{99m}Tc-sestamibi scan). While both scans (left panels) are negative for parathyroid adenoma, SPECT/CT imaging (right panel) enabled to identify abnormal tracer uptake located posteriorly to the trachea. (B) Two patients in whom SPECT/CT imaging with ^{99m}Tc-sestamibi localized hyperfunctioning parathyroid adenomas and led to plan the optimal surgical approach for their successful resection. In Pt #1 the adenoma was located adjacent to the right wall of the trachea, while in Pt #2 the adenoma was located in the anterior mediastinum.

An early report by Gayed et al. suggested that SPECT/CT had a significant impact on surgical management of patients in only a limited fraction of patients (5 out of 48 cases in their experience), and considered therefore that the added value of CT (with the related radiation exposure) did not justify the routine application of the procedure, except perhaps in patients with ectopically located adenomas [99]. However, more recent reports emphasize the impact of SPECT/CT compared to planar and/or SPECT scintigraphy (either as a stand-alone imaging or as side by side viewing with the corresponding CT images) on surgical

management of patients. This conclusion has been reached by Krausz et al. who report a change in the surgical approach in 10/33 ectopic and 4/23 orthotopic parathyroid adenomas [100].

Similarly, Serra et al. have shown that SPECT/CT improves preoperative localization of parathyroid adenomas, with significant surgical impact in 39% of the cases [101]. In their patients, SPECT alone correctly localized 14/23 parathyroid adenomas (61%), while SPECT/CT correctly localized all 23 lesions (100%, 14 of which were ectopically located). Furthermore, SPECT/CT was crucial in demonstrating the retrotracheal location of an adenoma in three patients. Better performance of SPECT/CT versus planar or stand-alone SPECT has also been reported by Lavely et al. [102], while Ruf et al. have emphasized in particular the role of SPECT/CT for attenuation correction of the SPECT data based on the CT transmission data [103].

In conclusion, image fusion as obtained by hybrid SPECT/CT imaging with ^{99m}Tc-sestamibi is of value for surgical planning in both primary and secondary hyperthyroidism [104]. Concerning in particular secondary hyperparathyroidism, it is crucial that all parathyroid tissue showing ^{99m}Tc-sestamibi uptake is removed, because these parathyroid glands are those responsible for the increased production of parathyroid hormone. When relying only on visual inspection of the surgical field, in the absence of functional information some simply hyperplastic (but not hyperfunctioning) parathyroid glands might be removed unnecessarily. Wider clinical expertise using the hybrid SPECT/CT technology will certainly have a relevant impact in this field.

3.12. SPECT/CT for diagnosing infection and inflammation

Infection and inflammation can represent a major diagnostic challenge for physicians. Diagnosis and precise delineation of infectious foci may be critical in certain clinical scenarios and render decisions concerning further patient management problematic [105, 106].

Both morphologic and functional imaging modalities have been extensively employed for diagnosing and monitoring infections. CT and MR images provide high-quality anatomic details. However, the structural abnormalities underlying the infectious process are, in some cases, non-specific or appreciable only in a subacute or late phase of the disease. Nuclear medicine has gained a crucial role in the evaluation of patients suspected of harbouring infection, especially because of its capability of demonstrating physiologic processes and metabolic changes that often precede anatomic changes by several days or even weeks [106–123].

Although a variety of new radiopharmaceuticals have been explored as to their ability to detect and localize infectious and inflammatory processes, ^{67}Ga-citrate scintigraphy and scintigraphy with ^{111}In- or ^{99m}Tc-HMPAO labelled autologous white blood cell (WBC) remain the functional imaging techniques of choice for diagnostic work-up of infection [105].

However, both ^{67}Ga-scintigraphy and WBC-scintigraphy suffer from poor spatial resolution and somewhat low specificity because of the absence or paucity of anatomic landmarks. These limitations make precise localization and characterization of areas with focal abnormal tracer uptake problematic, even when employing SPECT imaging. At least part of these difficulties can be overcome when contemporary CT images are available, by either side by side viewing

and, even better, by software based image fusion analysis [124, 125]. However, similar as with other scintigraphic applications, the introduction into clinical routine of integrated SPECT/CT scanners for combined anatomic and functional imaging has offered new opportunities for infection imaging, especially for facilitating precise anatomic localization and accurate characterization of infectious foci [2].

Recent reports have explored the contribution of SPECT/CT to a more accurate interpretation of WBC-scintigraphy for an array of clinical indications in different regions of the body, by distinguishing normal physiologic distribution of labelled WBCs from accumulation due to underlying infection. Major advantages have been observed for infectious processes with thoracic or abdominal localization, because of the potential difficulty of characterizing foci of WBC accumulation near the major vessels. In such cases, the hybrid technology helps in discriminating blood-pool activity from infectious sites, with substantial benefits for the evaluation of suspected vascular graft infection and fever of unknown origin [126].

Moreover, SPECT/CT with ^{99m}Tc-HMPAO-WBC can be very useful to image bone and joint infections, by allowing accurate localization of labelled WBC accumulation. In particular, in some cases of bone infection with adjacent soft-tissue involvement, while planar images alone are not able to distinguish soft tissue from bone, hybrid imaging is able to localize additional sites of leukocyte uptake in neighbouring soft tissue and to precisely define the extent of infection, thus modifying clinical patient management and therapeutic approaches in several cases.

After traumatic injury, skeletal changes can often be observed in morphologic imaging (i.e. CT or radiography). Although fusion imaging with a hybrid camera can improve the diagnostic accuracy of SPECT, it cannot be a substitute for conventional high resolution CT, which maintains its diagnostic role in most clinical situations. However, with regard to bone imaging, reports show that even the low-dose CT of the hybrid device may provide sufficient diagnostic anatomic information.

In this regard, Filippi and Schillaci have recently evaluated the usefulness of SPECT/CT for interpreting ^{99m}Tc-HMPAO-WBC scintigraphy in 15 patients with suspected osteomyelitis and 13 patients with suspected infection of orthopaedic prosthesis [127]. SPECT/CT fusion correctly characterized and localized the site of labelled WBC uptake in all patients with osteomyelitis, discriminating soft tissue from bone and having a substantial impact on the clinical management. Moreover, among patients with suspected infection of orthopaedic implants, SPECT/CT offered a more accurate anatomic localization of the site of infection than SPECT alone allowing differentiation between prosthesis and soft-tissue uptake. The authors concluded that hybrid imaging provided additional anatomic information on all patients with positive scan results (64.2%) leading to a more accurate definition of the extent of infection with significant impact in decisions therapeutics. In particular, major benefits were achieved for the diagnosis of relapsing osteomyelitis in patients with structural bone abnormalities after trauma.

Although ^{67}Ga-citrate has been used for scintigraphic imaging of infection and inflammation for many decades, its bio-distribution (with high accumulation in the gastrointestinal tract) and its sub-optimal physical emission characteristics result in a relatively poor imaging quality, making interpretation of abdominal imaging quite problematic. In an attempt to improve the quality of ^{67}Ga-citrate imaging, Bar-Shalom et al. have explored the added value provided by hybrid SPECT/CT imaging as an adjunct to ^{67}Ga-scintigraphy (in 47 patients)

and to ^{99m}Tc-HMPAO-WBC scintigraphy (in 31 patients) [126]. The contribution of SPECT/CT was analysed on a patient- and site-basis and was compared for the two tracers and for various clinical indications. SPECT/CT provided an additional contribution for diagnosis and localization of infection in 48% of the patients and in 47% of the sites. Although SPECT/CT, because of its capability to localize abdominal uptake within the bowel, enabled the correct exclusion of infection in four patients undergoing ^{67}Ga-scintigraphy, the investigators found that the clinical added value of SPECT/CT was significantly higher for WBC-scintigraphy than for ^{67}Ga scanning (63% versus 36% of patients). This data can be explained by the high specificity of WBC, with low background activity and therefore limited anatomic information.

New agents such as radiolabelled anti-granulocyte monoclonal antibodies, radiolabelled ciprofloxacin, radiolabelled biotin, may benefit from hybrid imaging, as reported in some preliminary studies. Biotin (or vitamin H) is utilized by growing bacteria at the site of infection according to the rate of their metabolism. This feature is the basis for the successful utilization of ^{111}In-biotin for imaging infection, especially in difficult to interpret conditions such as the spondylo-discitis. However, since Biotin does not appreciably accumulate in normal bone and/or bone marrow, the exact identification of the vertebral body harbouring infection can be problematic. Therefore, in order to improve diagnostic accuracy and to differentiate between vertebral and soft tissue paravertebral infection, SPECT/CT acquisitions may be performed. In a preliminary study, Lazzeri et al. have investigated the role of ^{111}In-biotin SPECT/CT in 70 patients with suspected spinal infection [128], and have thus confirmed the high diagnostic potential of one-step ^{111}In-biotin hybrid imaging. Moreover, these authors demonstrated that SPECT/CT imaging allows accurate evaluation of spinal infection differentiating between vertebral and soft tissue paravertebral involvement.

Other radiopharmaceuticals, such as ^{99m}Tc labelled anti-granulocyte antibodies (AGA), are known to be highly sensitive and specific for diagnosing infectious disease, but image analysis and exact anatomical definition of the infectious foci is often difficult. In a series of 27 patients with suspected chronic post-traumatic osteomyelitis, Horger et al. have evaluated the value of fused SPECT/CT imaging after injection of ^{99m}Tc-AGA [129]. All patients underwent planar and SPECT/CT imaging studies 4 h and 24 h after injection. The authors found high sensitivity (100%) for both planar and SPECT/CT imaging, associated however with different results in terms of specificity (78% for planar versus 89% for SPECT/CT). SPECT/CT correctly localized all abnormal foci of tracer uptake detected on planar and SPECT images, and also enabled accurate discrimination between soft-tissue infection, septic arthritis, and osteomyelitis.

Although the potential of fused SPECT/CT imaging in infectious and inflammatory disease has not yet been fully elucidated and further validation is required, hybrid imaging provides precise anatomic localization with significantly improved diagnostic accuracy over planar or SPECT alone (Figs 12–14). These new techniques, in conjunction with the use of highly specific radiotracers for detection of inflammatory disease, are creating a whole new and powerful armamentarium for diagnosing infectious foci.

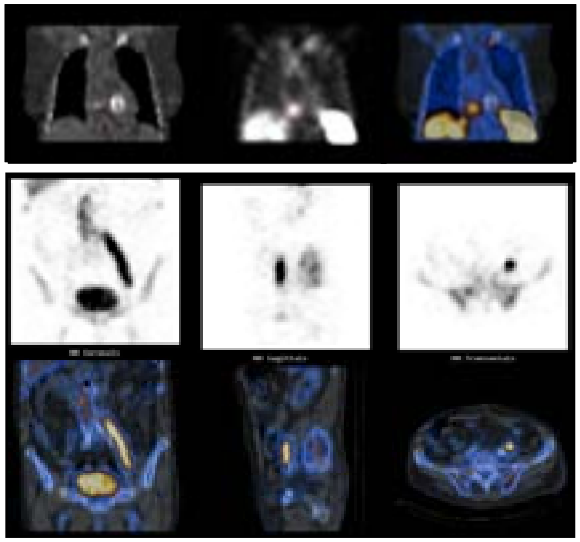

FIG. 12. Patients with cardiovascular infection imaged with autologous ^{99m}Tc-HMPAO-leukocytes and SPECT/CT. Although the most likely site of endocardial infection in Pt # 1 was expected to be a mitral valve implant (visible on the CT component of the examination), SPECT/CT correctly identified the tricuspidal valve as the actual site of infection (top panel). In Pt #2 (previously submitted to implant of aorto-bis-iliac vascular prosthesis), SPECT/CT defined the extent of infection as involving only the left side of the vascular graft (bottom panel).

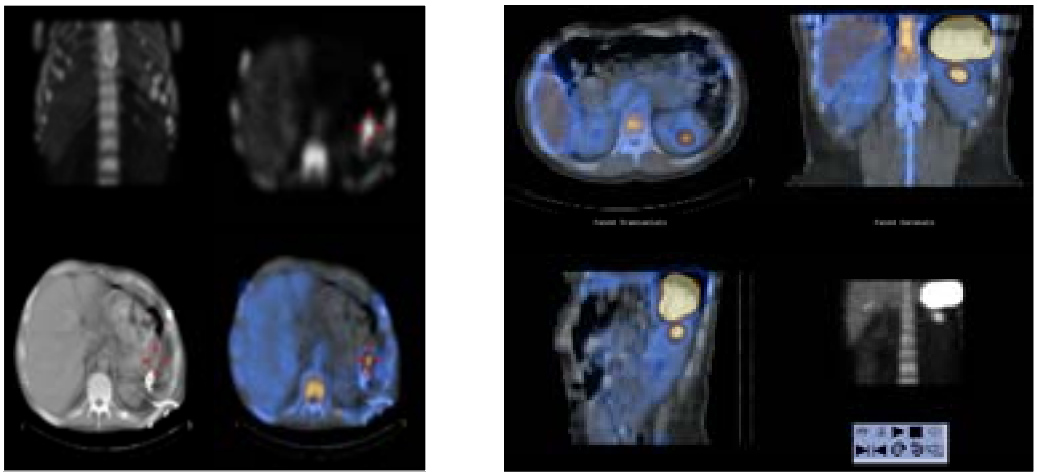

FIG. 13. Patients with infectious foci in the abdominal area. Pt # 1 (left panel) developed persistent fever resistant to antibiotic treatment shortly after combined pancreasectomy and splenectomy, performed because of a pancreatic adenocarcinoma of the tail infiltrating the splenic hilus. SPECT/CT performed as part of autologous ^{99m}Tc-HMPAO-leukocyte scintigraphy reveals a sub-diaphragmatic abscess at the tip of the draining catheter that had been placed during surgery. Pt #2 (right panel) had instead fever of unknown origin. During autologous ^{99m}Tc-HMPAO-leukocyte scintigraphy, it is only SPECT/CT that reveals location of an abscess at the upper pole of the left kidney, which on planar scan could only be generically located below the lower pole of the spleen.

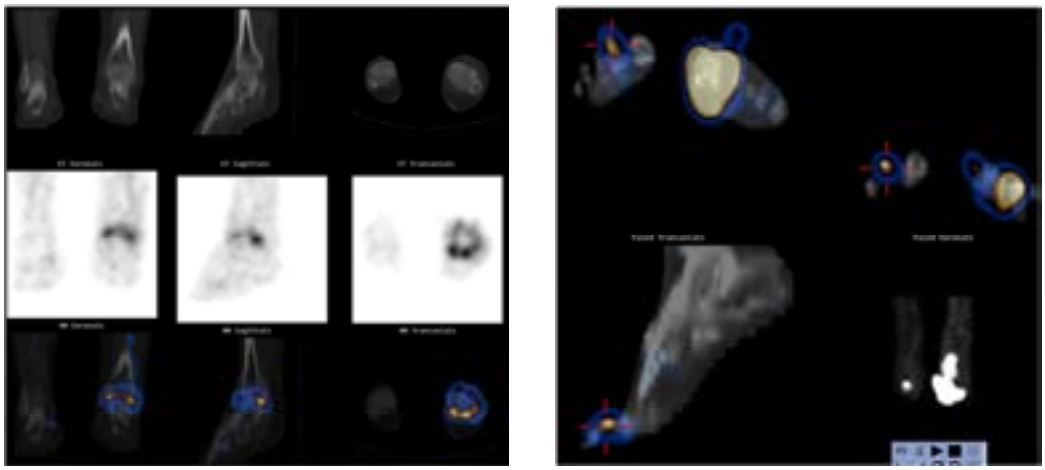

FIG. 14. Patients with different forms of osteomyelitis, with accurate definition of the extent of infection by SPECT/CT. Post-traumatic osteomyelits of the left ankle in Pt #1 (left panel), imaged after injection of ^{99m}Tc-anti-granulocyte antibody. In Pt #2 (right panel) SPECT/CT performed during autologous ^{99m}Tc-HMPAO-leukocyte scintigraphy demonstrates that infection arising in a diabetic foot involves not only the soft tissue but also bone structures. Such accurate localization of the disease process was problematic not only on planar scintigraphy but also on stand-alone SPECT.

3.13. Cardiac SPECT/CT procedures

3.13.1. Myocardial perfusion imaging — CT based attenuation correction

Myocardial perfusion imaging (MPI), using ^{201}Tl and ^{99m}Tc labelled radiopharmaceuticals for stress/rest SPECT studies is at present the main non-invasive modality for evaluation of coronary artery disease [130]. Its accuracy is, however, limited by image artefacts that can cause false–positive perfusion defects and therefore reduce the test specificity. Although the initial validation of MPI-SPECT performed in luminary sites reported a specificity of greater than 90%, further large-scale clinical use of the technique has been associated with specificity in the range of 60% or lower [131, 132]. One of the most common image artefacts is caused by non-uniform reduction of photon activity from attenuation by soft tissue. This can be recognized, or at least suspected by experienced readers, because of the typical location and shape relative to the heart. Attenuation artefacts usually occur in the anterior wall in women with large breasts and in the inferior wall in obese men [133–135]. Although the true prevalence of soft tissue artefacts is unknown, estimates range between 20% and 50% of patients [136, 137].

Several approaches have been used to address the issue of spurious false positive results in MPI due to photon attenuation including, among other options, awareness of their potential occurrence and location, routine assessment of raw imaging data, comparative assessment of studies performed following a change in the patient's position (prone versus supine) and gated imaging which assesses wall motion. These approaches improve artefact recognition but they all have limitations. Although guidelines of the American Society of Nuclear Cardiology recommend that attenuation correction should be performed in all patients, there are clearly some patient populations that benefit more from this procedure, generally the largest-size patients. Depending on equipment availability and daily workload, the rest SPECT study is

used in some centres as the criterion for triage decisions for performing attenuation correction acquisition.

In order to determine the true radiotracer distribution in the myocardium, several techniques have been developed with the goal of generating patient-specific attenuation maps. Attenuation maps generated by transmission sources at the time of the scan have, until the last decade, been the most commonly used method of correction. Various transmission geometries have been adopted, including sheet, multiple lines, or scanning line sources, a fixed source positioned at the focal line of a fan-beam collimator, or a moving point source [138]. Commercial systems use mainly Gadolinium-153 (^{153}Gd, 100 keV) with a 100-day half-life, supplied at a maximum of 400–500 mCi/source. With decay of the source, a degradation in the attenuation map leads to a central underestimation of the true attenuation coefficients.

An additional approach has attempted to use anatomic images imported from CT, but has been limited by difficulties in correct matching of the morphologic and scintigraphic data sets since images are acquired on different systems, at different time points, with the patients lying on different stretchers. These limitations are, at least in part, overcome by near-simultaneous acquisition of MPI and CT on a single imaging device. Historically, SPECT/CT systems have been initially developed with the specific goal of achieving optimal CT based attenuation of myocardial perfusion scintigraphy.

Cardiac SPECT is performed using a dual-head gamma camera equipped with low energy, high resolution parallel hole collimators, and with the detectors at 90° to each other. The acquisition is performed over a 180° orbit during a period of 12–20 minutes. Dual isotopes acquisition uses ^{201}Tl for rest and ^{99m}Tc-sestamibi or ^{99m}Tc-tetrofosmin for stress, while single isotope acquisition uses the same isotope, ^{99m}Tc-sestamibi or ^{99m}Tc-tetrofosmin for both rest and stress. For ^{201}Tl, imaging energy windows of 30% and 20% for the 70 keV and 167 keV peaks, respectively, are used, while the energy window width for ^{99m}Tc is 20% for the 149 keV peak. Both the rest and stress SPECT studies are followed by a low-dose CT (20–30 mAs, 140 keV for the diagnostic CT, or 2.5 mA, 140 keV for a camera-mounted CT), which is used for photon attenuation correction of the scintigraphic data. The CT-attenuation correction study is performed only over the area of the heart, as defined by the operator. The patient is asked not to move during study progression, in order to obtain good co-registration between the emission and the transmission scans [139].

CT based attenuation correction has been shown to provide the most reliable and accurate high quality cardiac SPECT images through high resolution, high count-rate and low noise attenuation maps resulting in predictable uniform tracer activity in patients with a low likelihood of haemodynamically significant coronary artery disease. The CT based attenuation correction method can be successfully implemented with all clinical cardiac SPECT protocols, including same-day or 2-days rest-stress, single and dual isotope rest-stress procedures.

3.13.2. Cardiac SPECT/CTA for assessing the significance of coronary artery lesions

Stress/rest MPI is the established imaging modality for non-invasive diagnosis of presence, severity and extent of coronary artery disease (CAD), with high sensitivity and specificity. MPI determines the physiologic significance of angiographically borderline stenosis, and defines the presence of viable but dysfunctional, hypoperfused myocardium. MPI cannot, however, diagnose early atherosclerosis and often underestimates the extent of coronary artery disease. In addition, MPI does not provide accurate anatomical information, essential

prior to coronary revascularization procedures. The recently developed multi-detector CT (MDCT) technology characterized by high spatial, contrast and temporal resolution enables non-invasive CT coronary angiography (CTCA) and provides also accurate information regarding the structure and motion of the heart chambers. CT, however, does not predict the benefit of revascularization [140–142].

Cardiac SPECT/CT is a novel hybrid imaging technique that combines detailed anatomical information of coronary vessels (provided by CTCA) with physiologic information of myocardial perfusion and function (provided by MPI), through accurate spatial alignment of both data sets. This evolving modality has the potential to become the future imaging test of choice for non-invasive assessment of CAD [140–142].

While co-registration of separately performed CT and MPI may provide a very similar type of data, this process is difficult to implement beyond research purposes in dedicated centres, due to its logistical limitations. Single devices combining SPECT/CTCA data are characterized by ease of use and simple logistic set-ups, and have the potential of making cardiac hybrid imaging user-friendly and easy to plan, major factors in their future routine clinical use. SPECT/CT can provide accurate non-invasive diagnosis of the culprit coronary lesion, including its location and morphology, in conjunction with assessment of the physiologic significance of this lesion on myocardial function. SPECT/CT images precisely localize regions of impaired perfusion to the corresponding vascular territory. Cardiac SPECT/CTCA may prove of significance in a series of potential indications, which will however need to be proven by large, multi-centre studies. By allowing visualization of stenoses, the addition of CTCA to MPI can potentially eliminate one of the major reasons for false negative MPI results in patients with advanced 3-vessel disease, showing a balanced reduction of blood flow in all myocardial segments. On the other hand, by assessing the functional consequences of stenosis through its stress/rest MPI component, it may improve the performance of CTCA in patients with dense coronary plaques. CTCA results are often insufficient to guide patient management. A need for functional information will arise in many patients demonstrating anatomic coronary abnormalities on CT.

In summary, reliable attenuation correction of MPI-SPECT enhances significantly the clinical decision making process; decreases morbidity related to invasive procedures and also saves costs related to additional work-up induced by equivocal reports. High speed multislice coronary CT has a growing impact on assessment of patients with known or suspected coronary artery disease. Combined data regarding myocardial perfusion, calcium scoring and the presence or absence of coronary stenosis may, in future, enable better stratification of patients with or without ischemic heart disease. Referral algorithms will have to define patient groups that will benefit from hybrid SPECT/CTCA imaging of both myocardial perfusion and the anatomy of the coronary tree.

3.14. Added values of CT in patients with coronary artery disease

3.14.1. Coronary artery calcium

Calcium accumulates in the coronary arteries as a result of the body's response to contain and stabilize inflamed coronary plaques. Calcified plaque assessment correlates with pathologic assessment of the total amount of calcified plus noncalcified plaques [143]. The burden of coronary artery calcium (CAC) generally reflects an advanced stage of plaque development, and CAC serves as an indirect but proportional marker for global atherosclerotic burden. The CT based method of quantifying CAC was initially developed using electron-beam

tomography (EBT), but multi-slice CT provides measurements of CAC comparable to those derived from EBT [144].

The CAC score is derived using highly reproducible semiautomatic computer methods based on the product of calcified plaque area by the coefficient of its density. The score is calculated as the product of the CAC area by the peak Hounsfield unit (1 for 131–199 HU, 2 for 200–299 HU, 3 for 300–399 HU, and 4 for >400 HU). Visually, coronary calcification can be categorized into mild (minimal), moderate, and marked (extensive) degrees of severity.

Accumulation of CAC is common in adults and increases with age. The presence of CAC is often associated with only insignificant (<50% luminal narrowing) coronary stenosis. However, there is a graded relationship between the extent of CAC and the annual risk of coronary heart disease. Patients with extensive CAC are likely to have marked non-calcified plaques that may be rupture-prone. Plaque erosions are infrequently calcified and associated with acute coronary syndromes [145].

3.14.2. Coronary computed tomography angiography

Coronary computed tomography angiography (CTA) visualizes not only the coronary vessel lumen but also the wall, allowing the non-invasive assessment of the presence and, potentially, the size of non-calcified coronary plaque. Furthermore, the assessment of ventricular function is possible from a single first-pass acquisition of the chest CT data, which may be of value in the emergency department setting, along with the potential to provide assessment of pulmonary embolism, acute coronary syndrome, and aortic dissection in a single study.

The relative roles of myocardial perfusion SPECT and CTA have not yet been defined. In patients with intermediate likelihood of CAD, coronary CTA may be the initial test to perform, attending to the apparently superior sensitivity over SPECT imaging. When a coronary CTA is entirely normal, no further testing would be required. In case of proximal and critical coronary stenoses, invasive coronary angiography would be indicated for possible revascularization therapy. When CTA detects coronary lesions of uncertain significance, SPECT imaging would be appropriate for further diagnostic assessment.

In patients with known disease (or likely having extensive coronary calcium) in whom risk-stratification is needed, SPECT imaging would remain the initial test.

If SPECT imaging has been performed as the initial test, further testing by CTA would be indicated whenever discordant results are obtained. This includes patients with a strong clinical suggestion of CAD after a normal or equivocal SPECT; patients with marked discordance between SPECT and clinical or stress ECG; or patients with SPECT and stress ECG results suggestive of left main or triple-vessel CAD (e.g. transient ischaemic dilation, post-stress LV dysfunction, exercise hypotension with normal SPECT), with balanced reduction of coronary flow in the LV. Coronary CTA can also be of use in patients with suspected nonischaemic cardiomyopathy, patients with coronary anomalies, and young patients undergoing valvular surgery.

Since rest/stress SPECT studies can be performed as routine in conjunction with coronary CTA, SPECT/CT systems provide data about coronary calcium, coronary stenosis and functional significance in one clinical setting, thus allowing more appropriate selection of patients who may benefit from revascularization procedures [146]. A recent study with an

experimental SPECT/CT scanner (16-MSCT) showed that integrated functional and anatomic results improved specificity and positive predictive value to detect haemodynamically significant CAD in patients with angina pectoris [141]. The sensitivity, specificity, positive predictive value, and negative predictive value of CTA were 96%, 63%, 31%, and 99%, respectively, as compared with 96%, 95%, 77%, and 99%, respectively, for SPECT/CT. Patients and arterial segments excluded from the analysis raised to 21% and 23%, respectively. Another investigation described the incremental diagnostic value of integrating SPECT/CT (64-MSCT) data through three-dimensional (3-D) image fusion on the functional relevance of coronary artery lesions [140]. 3-D volume-rendered fused SPECT/CT images were generated from patients with at least one perfusion defect on SPECT imaging, and compared with the findings from the side by side analysis with regard to coronary lesion interpretation by assigning the perfusion defects to their corresponding coronary lesion. In addition to being intuitively convincing, 3-D SPECT/CT fusion images added significant information on pathophysiological lesion severity in 22% of coronary stenoses of 29% of patients. Among equivocal lesions on side by side analysis, the fused interpretation confirmed haemodynamic significance in 35% of lesions and excluded functional relevance in 25% of lesions. In 7.5% of lesions, assignment of perfusion defect and coronary lesion appeared to be reliable on side by side analysis but proved to be inaccurate on fused interpretation. Added diagnostic information by SPECT/CT was more commonly found in patients with stenoses of small vessels and involvement of diagonal branches.

3.15. Pulmonary artery imaging in pulmonary embolism

Pulmonary embolism (PE) is one of the greatest diagnostic challenges in emergency medicine. It should be suspected in any patient with unexplained dyspnea, tachypnea, or chest pain. A negative D-dimer assay reliably excludes PE in low-risk patients. Otherwise, pulmonary CT angiography is now considered by several authors to be the initial imaging study of choice for stable patients. Nevertheless, ventilation/perfusion (V/Q) scans or even perfusion scintigraphy alone (as in the PISA-PED approach [147–152]) still retain a considerable diagnostic accuracy and are valid alternatives to pulmonary CT angiography, in particular when CT is not available, or in patients with contraindications to CT scanning or intravenous contrast.

The results of the Prospective Investigation of Pulmonary Embolism Diagnosis (PIOPED) study established the diagnostic criteria of V/Q scanning for the diagnosis of PE, as compared with pulmonary angiography [153]. The interpretation ranges from normal to high probability, each with its own diagnostic characteristics. However, more than 60% of patients fell into the low and intermediate probability (or non-diagnostic category), and there was a 4% incidence of PE when the scan was read as normal. Similarly troubling, high probability scans were associated with a 12% false positive rate [153]. Therefore, it is recommended to consider patients with low-to-moderate pretest probability and a normal V/Q scan as not having a significant PE. Nevertheless, if the same patients have a non-diagnostic V/Q scan, the recommendation is that, in order to exclude significant PE without going to pulmonary angiogram, the patient must have a negative whole blood D-dimer, negative bilateral ultrasound in low probability group, or negative serial bilateral ultrasound for the moderate probability group. In patients with high pretest probability a normal V/Q scan can only rule out PE if the patient has a normal chest X ray and no baseline cardiopulmonary disease. Otherwise, the patient must go on to CT angiography.

Because of the high number of indeterminate studies using V/Q scanning [153], pulmonary CT angiography (PCTA) is becoming the initial diagnostic test for PE for stable patients with

no signs and symptoms of deep venous thrombosis. PCTA with 100 ml of iodinated contrast medium and dedicated imaging procedures and protocols can directly visualize thromboembolic filling defects as well as pleural effusions, vascular remodelling, and oligoemia, any of which may be present with PE [154]. In addition, PCTA may reveal alternative diagnoses, such as pneumonia, aortic dissection, tumour or pneumothorax that in the absence of PE may yield a previously unsuspected reason for symptoms mimicking PE [155]. Current multi-slice CT scanners can image the entire pulmonary vasculature in one breath-hold, allowing 1 mm to sub-millimeter resolution, and the data can be transformed into 2-D and 3-D reconstructed images. Such procedure can significantly increase the detection of 'clinically significant' subsegmental thrombi and evaluate pulmonary vasculature down to 6^{th} order branches [156–158].

The PIOPED II study [159] recently reported the high accuracy of multi-slice CT scanners for the diagnosis of PE, with 83% sensitivity, 96% specificity, 95%, 89% and 60% negative predictive values, as well as 96%, 92% and 58% positive predictive values, respectively for high, intermediate, and low clinical probability groups. These data support the use of PCTA for suspected PE as a stand-alone imaging technique in most patients. However, the false negative rate of 17% should be noted. The most likely explanation for this is that multi-slice CT scanners (mainly 4 slice) still miss small, peripheral subsegmental clots that are better detected by V/P scanning or by classic pulmonary angiography. Therefore, clinicians should be cautious with results that are discordant with their clinical judgment, particularly in front of a normal PCTA in a patient with a high clinical probability of PE [160].

While the clinical significance and treatment requirements of small, peripheral subsegmental thrombi are controversial [161], image fusion of SPECT V/Q and PCTA has demonstrated to be feasible. A recent investigation in 30 consecutive patients who underwent both imaging studies during their admission for investigation of potential PE reported good accuracy of co-registered images as determined subjectively by correlation of the anatomical boundaries and co-existent pleuro-parenchymal abnormalities [160]. Nine patients who had positive PCTA performed as an initial investigation had co-localized perfusion defects on the subsequent fused PCTA/SPECT images. Three of the 11 V/Q scans initially reported as intermediate probability could be reinterpreted as low probability owing to co-localization of defects with parenchymal or pleural pathology [162]. Therefore, the introduction of SPECT/CT hybrid systems will probably provide a single diagnostic tool that will overcome limitations of each imaging modality separately.

4. ADVANTAGES OF UTILIZING SPECT/CT

4.1. Anatomical accuracy of image registration in SPECT/CT hybrid imaging

Image registration is defined as the transfer of two image data sets into one common coordinate system. It may be mono or bimodal, i.e. between images acquired by one single modality or by two different modalities. Depending on the nature of the transformations used, rigid or non-rigid approaches can be used for this purpose, the former allowing for non-linear, 'plastic' deformation of the image data sets. A further distinction can be made between software based registration of data sets acquired independently one from each other by two different imaging devices and hardware based registration where the two data sets are obtained by hybrid equipment in a single imaging session.

In the past decade, the clinical impact of interactive software based registration between SPECT and CT data has received some attention in the literature [163, 164]. In particular, it has been repeatedly demonstrated that patient management may benefit significantly from the integration of functional and morphological data.

One major drawback of software based image fusion is logistic in nature: in the daily clinical routine of many institutions, image data sets from different modalities can be exchanged between different departments only with some difficulty. Although the implementation of hospital-embracing picture-archiving systems should overcome these difficulties, software based registration suffers from anatomical inaccuracies stemming from different positioning of the patient in the two separate imaging devices as well as by difficulties in identifying landmarks common to both data sets to be registered. In addition, the more specific a radiopharmaceutical is for a certain tissue, the poorer images of its distribution are with regard to anatomical detail, and the more difficult software based registration becomes.

These limitations are greatly reduced in hardware based registration that should therefore offer a higher anatomical accuracy of image fusion, as it obviously emerges when reviewing articles investigating the quality of alignment between [^{18}F]FDG-PET and CT. In these studies, anatomical accuracy of fusion is usually quantified by determining the average distance between landmarks or lesions identifiable on both images. This distance ranges between 4 and 12 mm for software based fusion of PET and CT images [165–169], but is reduced 3–5 mm for PET/CT hybrid scanning [168, 169], thus confirming the assumption of a higher anatomical accuracy for hybrid imaging.

Nevertheless, similar data for registration between SPECT and CT images are scarce. Förster et al. studied the accuracy of software based fusion between ^{111}In-octreotide SPECT and multi-row CT in a small group of patients [44]. They reported anatomical inaccuracies in the range of 7 mm, similar to those determined for fusion between PET and CT. Nömayr et al. reported a much higher accuracy of image fusion for SPECT/CT hybrid imaging of the lower lumbar spine [170]. In their study, misalignment ranged between 0.7–1.8 mm, smaller than pixel width in the SPECT images. Notably, software based registration performed on the data sets acquired by SPECT/CT could still significantly improve these results and bring misalignment down to values averaging 1 mm. However, their results cannot be extrapolated to regions of the human body involved in respiratory movements affecting SPECT and CT images to a different degree.

The development of hybrid imaging devices witnessed in the last decade marks a new trend in medical imaging involving the registration and fusion of all image data sets of one individual patient using the same computer platform. Current available data has already proven a major clinical impact of this approach, which is also expected to increase cost effectiveness. The field will be driven by the development of new hybrid imaging devices, but also by significant improvements of software based image fusion. Future medical imaging departments will offer a multimodal environment integrating both hybrid imaging and software based image fusion into the daily clinical routine.

4.2. The effects of CT based attenuation correction of SPECT image data sets and potential future applications

Attenuation artefacts considerably degrade the quality of SPECT images, and also hamper accurate quantification of tracer accumulation in specific volumes of interest. Various methods of attenuation correction have been proposed [171, 172], to be further subdivided

into those with and those without transmission measurements. The latter calculate tissue attenuation coefficients on the basis of an assumption of their distribution in the body segment examined, using various methods to determine the body outline. This approach is widely used in studies of brain perfusion, since it is generally assumed that attenuation is homogeneous within the skull.

This assumption does not hold valid for the abdomen or the chest, since these body segments contain tissues with variable attenuation coefficients. Radionuclide transmission scanning has been used to derive maps of abdominal and thoracic attenuation coefficients. However, it has been repeatedly shown that this approach can introduce artefacts that may be difficult to identify [173]. Another major problem inherent to this approach is the low activity of the radioactive sources used for this purpose, leading either to long acquisition times or to attenuation maps with poor quality due to low counting statistics.

This problem is overcome by employing CT data to correct SPECT data for tissue attenuation. A study investigating the visualization of radioactivity in a heart phantom has indeed shown that this variable is homogenized by CT based attenuation correction [174]. Recently, Fricke et al. have demonstrated that the concordance between PET and SPECT studies of myocardial perfusion was improved after using CT based attenuation correction for the SPECT data [175]. Similar results have been reported for skeletal SPECT [176].

Nevertheless, the clinical impact of CT based attenuation correction for SPECT imaging is currently unclear. In a multi-centre trial, Masood et al. demonstrated a moderate, but statistically significant increase in the accuracy of diagnosis of coronary artery disease for myocardial perfusion SPECT [174]. Shiraishi et al. reported a significantly higher accuracy for attenuation-corrected ^{201}Tl-SPECT in staging lung cancer compared to the non-attenuation studies [177]. Likewise, improved identification of sentinel lymph nodes has been shown with the use of attenuation correction [60].

When using CT based attenuation correction for SPECT data, one should be aware of possible artefacts caused by misalignment between SPECT and CT data sets (see above). Figure 15 demonstrates such an artefact in a phantom simulation. In myocardial perfusion SPECT, a 7 mm misalignment between emission and transmission data, corresponding to the width of one pixel in that study, was shown to produce a 15% change in relative regional activity [178]. Similar data have been published for CT based attenuation correction in myocardial SPECT [179] and a method for automated control for misalignment between CT and SPECT has been proposed [180]. In skeletal SPECT, misalignment of the CT by 1 cm was shown to change even the visualization of symmetry of uptake [176]. Therefore, the anatomical accuracy of fusion should be carefully checked before applying CT based attenuation correction.

Attenuation correction of SPECT data constitutes an important step in the development of truly quantitative SPECT, which may improve dosimetric estimates of molecular radiotherapy. More sophisticated phantom studies are needed to better understand variability related to different photon energies. However, for accurate SPECT, quantitation issues related to scatter and partial volume artefacts need to be overcome. In particular, the correction of the latter could also capitalize on the use of CT images aligned to SPECT. Therefore, the new hybrid systems will stimulate research work also along that avenue.

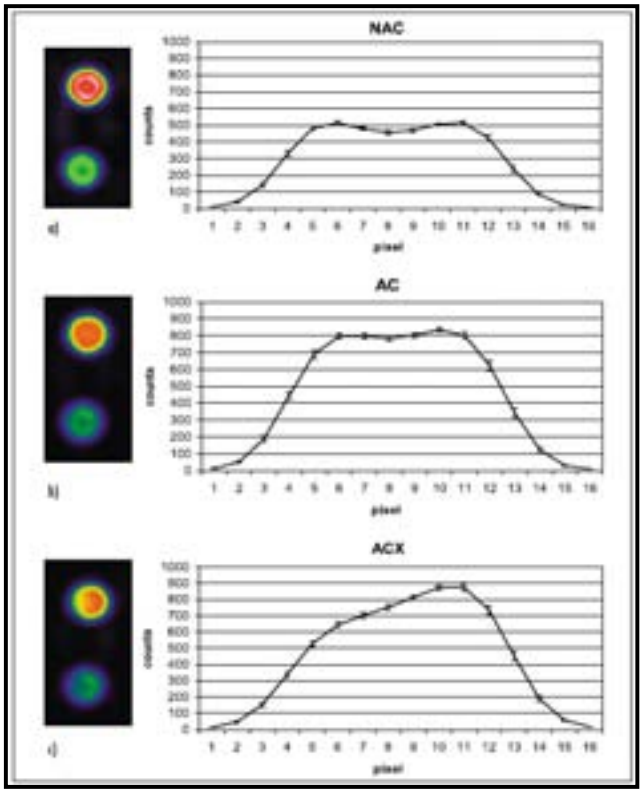

FIG. 15. Transversal SPECT images of two rods in a phantom filled with ^{99m}Tc (a) without (NAC) and (b) with attenuation correction (AC): attenuation correction homogenizes the visualization of activity in the homogeneously filled rods; (c) a CT misalignment by 1 cm in X-direction (ACX) produces a significant artefact in the visualization of activity. The curves are profiles from left to right for the rod filled with the lower activity concentration in NAC, AC, and ACX (from TKL31; with permission).

4.3. Additional information or diagnosis from CT

With continuous higher-speed and thinner sliced CT, small lung lesions (less than 1 cm in diameter) showing interval increase in size may often be detected. Small non-specific lymph nodes, low-density hepatic or renal lesion, and osteolytic or osteoblastic lesion with interval increase in size are also incidentally identified. These lesions are generally beyond the resolution of our current SPECT or PET system and may require further short term follow-up studies to confirm/exclude the diagnosis of new metastases.

4.4. Use of SPECT/CT data for estimating internal radiation dosimetry

As will be better detailed in the next section, the radiation dose is energy absorbed per unit of mass. Accurate dosimetric estimates are extremely critical in radiometabolic therapy, both for calculating radiation dose to the target organ/tissue (generally tumour, but also non-tumour lesions such as hyperfunctioning thyroid parenchyma) and for defining dose-limiting toxicities to normal organs/tissues with high physiologic accumulation of radioactivity (e.g. bone marrow, kidneys). It is well known that internal dosimetry estimates are burdened by a significant degree of estimation regarding absolute concentration of radioactivity in a given organ/tissue, and represent therefore only rough approximations with variabilities that can be

as high as 50% or even 100%. Part of this variability is due to the fact that bio-distribution data are usually derived from planar imaging (such as conjugated-view whole body scans), and a-priori models and assumptions on the organ shapes/sizes are employed for the radiodosimetric analysis. Also stand-alone SPECT entails some unwarranted assumptions, since standard factors are usually applied for attenuation correction. In this regard, SPECT/CT certainly holds the promise for developing more accurate approaches to internal radiation dosimetry estimates, since the CT component of the study enables correct attenuation of the emission map specifically in each single patient.

Few reports have been published on this important application of SPECT/CT. Boucek and Turner employed SPECT/CT data to estimate bone marrow dosimetry following the administration of ^{131}I labelled anti-CD20-monoclonal antibody (rituximab) in patients with non-Hodgkin's lymphoma. These patients are usually heavily pretreated with chemotherapy, and myelosuppression is the dose-limiting toxicity. The authors demonstrated a statistically significant correlation ($p = 0.001$) between whole body effective half-life of the radiolabelled antibody and effective marrow half-life. They also found that bone marrow activity concentration was proportional to administered activity per unit weight, height or body surface area ($p < 0.001$). In their experience, SPECT/CT enabled accurate quantification of activity accumulations and thus validated patient-specific prospective dosimetric estimates methods [181].

SPECT/CT has also been advocated for the quantification of radiation doses delivered during radiometabolic therapy with ^{131}I-MIBG, using CT based tumour volume-of-interest [23]. Although based on a single patient, Song et al. have demonstrated that patient-specific 3-D dosimetry based on SPECT/CT is feasible and important in the dosimetry of thyroid cancer patients with radioiodine-avid lung metastases and prolonged retention in the lungs. In their opinion, this procedure could constitute the breakthrough for rationally planning radionuclide therapy in patients with thyroid cancer [182].

A preliminary report from the Pisa group described a novel SPECT/CT based approach to calculate attenuation- and scatter-corrected dosimetry to the bone marrow and to tumour lesions following the administration of ^{153}Sm-EDTMP for palliation of bone pain in patients with hormone-refractory metastatic prostate cancer [183]. The system was phantom-calibrated for tissue densities, and the CT images were utilized to identify bone structures. Dedicated software was developed for automatic edge recognition of skeletal uptake, which was corrected for attenuation and scatter. An S-value matrix was then derived from the attenuation map voxel-by-voxel for each individual patient (rather than pixel-by-pixel as in conventional evaluations) (Fig. 16). It was found that the conventional approach based on planar imaging and standard-factor corrections overestimated dose to bone marrow by an average 67% versus the SPECT/CT method. The new SPECT/CT based method therefore opens the perspective of calculating radiation dose to the bone marrow and to skeletal lesions (or other sites), and therefore to correlate dosimetry to lesions with efficacy of therapy (bone palliation, or true anti-tumour effect [184]).

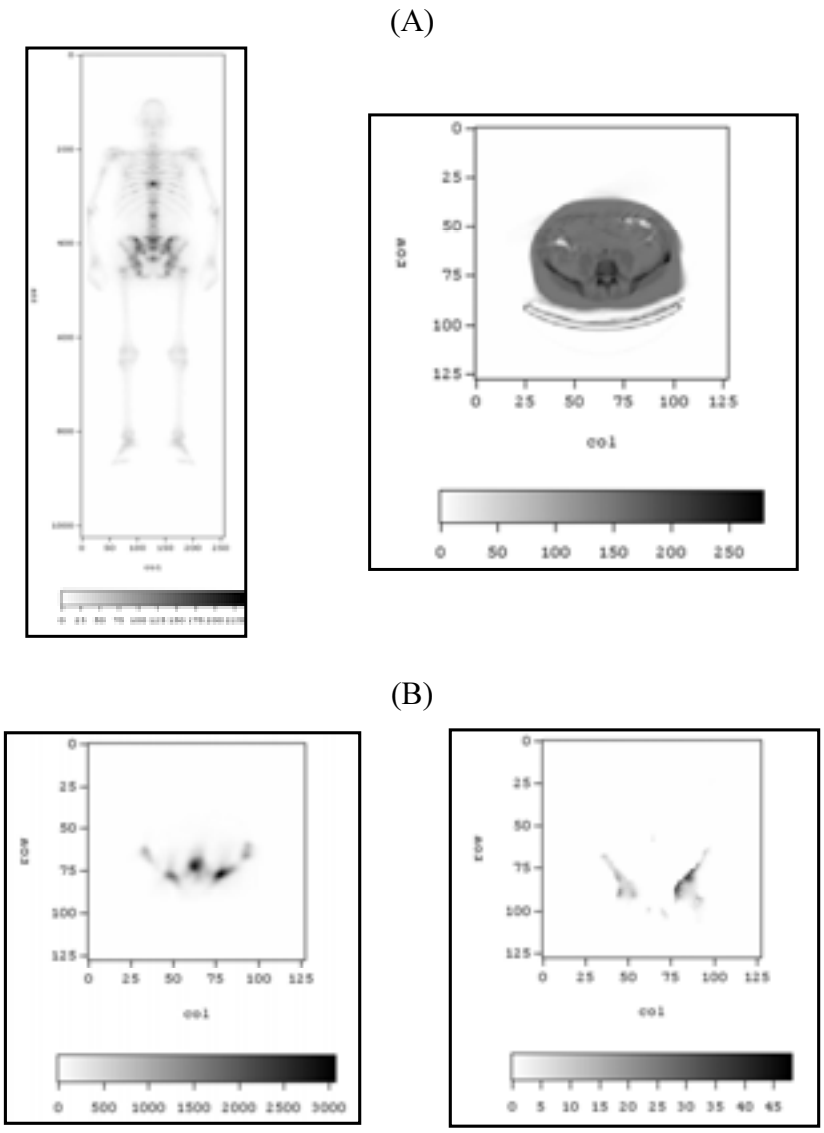

FIG. 16. Sequential steps in the elaboration of the SPECT/CT images obtained after administration of ^{153}Sm-EDTMP given for bone pain palliation purposes in a patient with hormone-refractory prostate cancer. (A) Outline of skeletal uptake of the bone-seeking radiopharmaceutical as derived from an automatic edge-recognition software applied on the planar 24 h whole body scan (left panel). The right panel shows the CT density-reconstructed map acquired at the pelvis. (B) Reconstructed SPECT map (left panel) and tomography of the 3-D dosimetry map in Gy (right panel).

4.5. Radiation dose of CT from SPECT/CT

The radiation absorbed dose delivered to the patient from the use of CT in SPECT/CT study is difficult to measure because of many factors involved, but the CT Dose Index (CTDI) based on scan parameters can be calculated, and represents an index of radiation dose to a standard phantom. The CT scanners generally provide an X ray tube current modulation function that makes uniform image quality and dose for various patient sizes [185]. The system will automatically increase or decrease the tube current (mA) when the user selects a reference effective mA in response to changes in diameter or tissue density of the patient. The effective mA includes the tube current, rotation speed, and pitch used for the scan. The user-selected

scan parameters that affect patient dose in CT examinations are effective mA, kVp, detector collimation setting (affecting the width of the radiation beam in table-travel direction), beam-shaping filter associated with the scan type (body or head), and number of scans over the same section of the body. If the dose distribution from the centre to the edge of the phantom as well as the pitch used in the scan is taken into account, a term called CTDIvol can be used to represent the dose index to the volume of the phantom. The radiation dose is energy absorbed per unit mass. The CTDIvol associated with a single CT scan covering one SPECT bed position is the same as the CTDIvol for a CT scan covering two non-overlapped SPECT bed positions if the same CT scan parameters are used. However, there is a factor of two variation in the radiation risk to the patient between these two cases. The CTDIvol in milli-Gray (mGy) is multiplied by the length of the CT scan in cm, to yield the dose-length product (DLP). Once the DLP is determined, an effective dose can be estimated using conversion factors for the relative radiosensitivity of the organs within the range of the scan. Some CT scanners save the CDTIvol and DLP values for a specific patient scan at the end of the examination. If there are multiple CT scans of the same region of the patient, each scan adds to the radiation dose and risk.

The effective dose and CTDIvol values from typical CT scans to the chest and abdomen have been calculated [186], and they are 4 mSv and 8 mGy, respectively. The value to the head and neck are 4 mSv and 10–20 mGy, respectively. These doses are for one SPECT bed position, relating to a 39 cm CT scan length, acquired using a fixed technique at the reference mA. Doses can be scaled linearly with the actual scan effective mA for the patient study. In case of a CT for a two-bed SPECT/CT, the appropriate effective dose values are added together. A planning CT view is obtained prior to determining the scan extent and location with low (about 20) mA for the postero-anterior projection and with the beam direction such that the beam enters the table prior to passing through the patient. These measures ensure an adequate planning view with the lowest dose to the patient, which is about the same as for a single view of the chest X ray.

5. FURTHER DEVELOPMENT OF SPECT/CT WITH NEW RADIOPHARMACEUTICALS

There is a continuous interest to label biologically important drugs or agents with easily available and cheaper isotopes than PET tracers, such as ^{99m}Tc labelled tracers (Table 1) for SPECT/CT to diagnose, differentiate, and stage cancers and also to evaluate as well as to predict therapeutic responses. L,L-ethylenedicystein, the most successful example of N_2S_2 chelates, can be labelled with ^{99m}Tc with high radiochemical purity, and the preparation remains stable for several hours [187]. Reliable molecular imaging that: assesses cellular targets at low cost, treatment response more rapidly, provides a good differential diagnosis, predicts correctly therapeutic response and allows for better radiation dosimetry for internal radiotherapy, would be very valuable.

6. CT TRAINING IMAGING FOR NUCLEAR PHYSICIANS AND TECHNOLOGISTS

The Societies of Nuclear Medicine, Computed Body Tomography and Magnetic Resonance, and the American College of Radiology have recently agreed that only properly trained qualified physicians should interpret PET/CT images [189]. The issue of training nuclear physicians to interpret the CT images produced by SPECT/CT devices is similar to that for

PET/CT. In this regard, earning 100 hours of CT continuing medical education credits and interpreting 500 CT cases under the supervision of qualified diagnostic radiologists were recommended. The CT cases should include reasonable numbers of head and neck, chest, abdomen and pelvis examinations. According to these recommendations, both radiology and nuclear medicine residents are required to interpret SPECT/CT images.

TABLE 1. SPECIFIC RADIOTRACERS [187, 188]

Character of cancer cells	Compounds
Cellular growth	^{99m}Tc-deoxyglucose ^{99m}Tc-guanine
Hypoxia	^{99m}Tc-metronidazole
Angiogenesis	^{99m}Tc-endostatin ^{99m}Tc-bevacizumab (against VEGF receptor)
Apoptosis	^{99m}Tc-annexin-V
Hormones	^{99m}Tc-estradiol

SPECT/CT and PET/CT present therefore similar practical issues regarding education, training and certification of nuclear medicine technologists to become properly qualified and competent to perform the CT portion of the study. The American Registry of Radiologic Technologists has adapted its CT certification examination and has allowed certified or registered nuclear medicine technologists who have met the required prerequisites to take this examination.

Nevertheless, the choice of the optimal way to achieve adequate training for interpreting multimodality imaging examinations will differ between countries owing to differences in infrastructure and legislation. The European Association of Nuclear Medicine (EANM) and the European Society of Radiology (ESR) have agreed to work together to produce a common position paper regarding multimodality imaging systems [190, 191]. Both organizations recognize the importance of coordinating working practices for multimodality imaging and that undertaking the nuclear medicine and radiology components of imaging with hybrid systems requires different skills. Training should be properly structured and comprehensive and should be conducted in accredited training centres. It should incorporate the principles and all modalities of both specialties to allow the trainee to acquire a full understanding of the possibilities and difficulties of each technique and its medical background, and provide the basis for participating in the evolution of multimodality imaging. Refresher type courses can prepare for specific training or refresh knowledge, but cannot replace appropriate on site training. It is not acceptable for training to be focused on a single technique.

Three different training models have been proposed [190]:

- Comprehensive training in both specialties, clinical radiology and nuclear medicine, in those countries where it is possible for the individual to practice both specialties and where such dual specialty training can be obtained. Such training gives the trainee the possibility of ultimately practicing in one or both of the specialties and of billing appropriately. The duration of the entire training programme in both specialties would most likely be neither politically nor economically acceptable in many European countries.

- An adequate period of training in the other specialty in addition to full training in the primary specialty. This model would facilitate acquisition by nuclear medicine specialists or radiologists of the necessary training in the other specialty after having completed full training in their primarily chosen specialty. Such adjusted additional training programme should be defined to provide a broad foundation of knowledge in the second specialty and should not be confined to a single technique such as CT or SPECT or a single clinical application. For nuclear medicine specialists, besides relevant radioprotection issues, training will include the physical principles and practical clinical skills of CT imaging. For radiologists, besides relevant radioprotection issues, training will include knowledge of radiopharmacy and radiotracer biokinetics and the physical principles and practical skills of SPECT. Training needs not to include therapeutic interventional radiology or radionuclide therapy. The core of the additional training would be dedicated to hybrid imaging. For radiologists, part of the nuclear medicine component should be undertaken during the fourth and fifth year of training. Maintenance of radiology skills during this time would be mandatory. For nuclear medicine specialists, part of the radiology component should be undertaken during the fourth and fifth years of training. Maintenance of nuclear medicine skills during this time would be mandatory. The remaining part of the training would then be obtained with an additional year fully dedicated to the second specialty, giving a total of 6 years' training for both specialties. The exact duration of the training is subject to local regulations, which may vary from country to country. Nonetheless, the general time scale as outlined in this option should be considered as the model. Such additional training will lead to a special competency certification.

- Potential future integration of training: an incorporated training in nuclear medicine and radiology taking the form of a cross-over or integrated training programme, where both specialties agree and recognize a training curriculum which encompasses the principles of all imaging modalities of both specialties. The curricula of both specialties would be adapted to include knowledge of anatomy, cell biology, genetics and physiology as well as the normal requirements of the physical basis of all imaging modalities and patient safety.

Each country should establish a training schedule that ensures the accomplishment of appropriate education in both specialties, bearing in mind that this cannot be achieved by merely performing a certain number of studies with one or the other technique. Only thorough training will give the necessary insight into anatomical and functional aspects of the various modalities, their interpretation with respect to patient-tailored treatment and risk assessment, and finally the further development and refinement of multimodality imaging.

During the interim period while these training models are set up, the nuclear medicine specialist would manage and report the nuclear medicine component of the examination and the radiologist would manage and report the anatomical and pathological component, with consultation between the two specialists to combine the data into a final diagnosis. Each specialist would provide a report with regard to the part of the study that he/she is directly responsible for. The benefit of this strategy is that those fully trained in the specific modalities would interpret the images jointly, thus providing a high-quality result. At a practical level this concept requires careful organization, cooperation and discussion between nuclear medicine and clinical radiology specialists.

7. REFERRAL CRITERIA FOR SPECT/CT

Local logistics and availability of different medical specialties dictate how diagnostic algorithms are applied in the clinical routine when patients are referred for diagnosis and/or characterization of their disease, and in particular to SPECT/CT. These examinations should be performed with the purpose of, whenever possible, avoiding the use of invasive procedures, when surgery is contemplated as part of treatment, or prior to adopting mini-invasive approaches. Clearly, a combined imaging technique such as SPECT/CT provides all the morpho-functional information enabling the surgeon to plan the surgical approach most suited to the individual patient. Referring clinicians have learned to regard radionuclide studies as useful tests that may confirm a suspected clinical diagnosis and characterize disease processes with information that can be relevant to treatment of the disease. This review has been designed to provide a summary of a methodological radionuclide based approach, SPECT/CT, a still evolving procedure with the final goal of enhancing diagnostic information and guiding therapy. It includes the methodology, analysis and estimation of usefulness of these examinations with an emphasis on more recently published data. Based on this review and on the experience accumulated by each centre represented in this panel of experts, referral criteria for a SPECT/CT examination can briefly be summarized in the indications that follow.

Indication to perform a SPECT/CT examination can be raised on primarily clinical ground. Such indications include:

- High suspicion for active disease, or known structural pathology, as SPECT/CT may localize multiple sites and define extent of disease;
- Planning treatment (medical, surgical, or radiation therapy);
- Monitoring response to treatment.

In some other cases, indication can also originate on the basis of data from previous anatomic imaging, including situations such as:

- Abnormal structural findings of equivocal functional significance, either at diagnosis or post-treatment;
- Absence of overt structural pathology in the presence of high clinical suspicion.

It is sometimes necessary to clarify inconclusive results of prior functional imaging (usually planar scintigraphy), showing foci of increased radiotracer uptake of unclear localization and clinical significance. Inconclusive scintigraphic studies can be due to tracer-related factors (because of poor physical characteristics, high target-specificity with paucity of non-target anatomic landmarks, physiologic bio-distribution with the lesion close to excretion sites). Alternatively, inconclusive radionuclide imaging can be due to patient/disease-related factors, such as complex regional anatomy or anatomic distortion post-treatment (surgical and/or radiation therapy).

Finally, emphasis should be placed on the use of the CT component of a SPECT/CT examination for correcting, on a patient-specific basis, the single photon emission data for attenuation and scatter. This is crucial for proper estimation of radioactivity concentration in specific organs/tissues on a volumetric basis.

8. CONCLUDING REMARKS

In summary, a high quality SPECT/CT study requires a reliable, well functioning hybrid scanner which has met acceptance testing criteria and which is regularly monitored for quality of performance. The study must be designed to answer the specific question asked by the referring physician, and the patient must be appropriately educated and compliant with the preparations for the scan, including fasting if so indicated. The technical staff must be well trained to perform and monitor both components of the study according to a well defined protocol. The acquisition and processing protocols must be carefully followed. The images must be reviewed for technical and diagnostic quality before the patient leaves the department. Finally, the images must be interpreted by skilled readers who are well aware of the clinical history of the patient, using workstations that allow integrated viewing of the functional and anatomic data. In this way, a high quality study will provide useful diagnostic information for further clinical management and patient care. As the quality of SPECT/CT devices improves, it is expected that new applications will emerge.

The impact on reader confidence and increased credibility with referring clinicians is an important add-on feature for SPECT/CT. The concept of incremental confidence is difficult to quantify. It is clear that evaluating the impact of combined SPECT/CT remains a subjective process. While nuclear medicine physicians interpret a study, referring clinicians often remain in doubt because of the difficulties visualizing the location of the finding on scintigraphy alone. Correlation with CT data through precise image registration makes the interpretation of high signal-to-background functional images, combined with better anatomic information, less dependant upon individual expertise. Thus, SPECT/CT results in more meaningful communication with referring physicians, as the hybrid imaging study interpretation is more credible to the clinician who is able to see the location of the functional, tracer-avid focus.

REFERENCES

[1] KEIDAR, Z., ISRAEL, O., KRAUSZ, Y., SPECT/CT in tumor imaging: technical aspects and clinical applications, Semin Nucl Med **33** (2003) 205–218.

[2] O'CONNOR, M.K., KEMP, B.J., Single-photon emission computed tomography/computed tomography: basic instrumentation and innovations, Semin Nucl Med **36** (2006) 258–266.

[3] MADSEN, M.T., Recent advances in SPECT imaging, J Nucl Med **48** (2007) 661–673.

[4] BAILEY, D.L., ROACH, P.J., BAILEY, E.A., et al., Development of a cost-effective modular SPECT/CT scanner, Eur J Nucl Med Mol Imaging **34** (2007) 1415–1426.

[5] ROACH, P.J., BAILEY, D.L., Combining anatomy and function: the future of medical imaging, Intern Med J **35** (2005) 577–579.

[6] RÖMER, W., NÖMAYR, A., UDER, M., BAUTZ, W., KUWERT, T., SPECT-guided CT for evaluating foci of increased bone metabolism classified as indeterminate on SPECT in cancer patients, J Nucl Med **47** (2006) 1102–1106.

[7] PARKIN, D.M., WHELAN, S.I., FERLAY, J., Cancer Incidence in Five Continents, Vol. 7, IARC Scientific Publication 143, International Agency for Research on Cancer, Lyon (1997).

[8] McDOUGALL, I.R., Thyroid Cancer in Clinical Practice, Springer, London (2007).

[9] SCHLUMBERGER, M., PACINI, F., Thyroid Tumors, Nucléon, Paris (2003).

[10] GREENE, F.I., PAGE, L.I., FLEMING, I.D., et al., AJCC Cancer Staging Handbook, Springer, New York (2002).

[11] GIMM, O., BRAUCKHOFF, M., THANH, P.N., SEKULLA, C., DRALLE, H., An update on thyroid surgery, Eur J Nucl Med Mol Imaging **29** Suppl. 2 (2002) S447–S452.

[12] THARP, K., ISRAEL, O., HAUSMANN, J., et al., Impact of ^{131}I-SPECT/CT images obtained with an integrated system in the follow-up of patients with thyroid carcinoma, Eur J Nucl Med Mol Imaging **31** (2004) 1435-1442.

[13] SHAPIRO, B., RUFINI, V., JARWAN, A., et al., Artifacts, anatomical and physiological variants, and unrelated diseases that might cause false-positive whole-body I-131 scans in patients with thyroid cancer, Semin Nucl Med **30** (2000) 115–132.

[14] PACINI, F., CAPEZZONE, M., ELISEI, R., CECCARELLI, C., TADDEI, D., et al., Diagnostic 131-iodine whole-body scan may be avoided in thyroid cancer patients who have undetectable stimulated serum Tg levels after initial treatment, J Clin Endocrinol Metab **87** (2002) 1499–1501.

[15] MAZZAFERRI, E.L., ROBBINS, R.J., SPENCER, C.A., et al., A consensus report of the role of serum thyroglobulin as a monitoring method for low-risk patients with papillary thyroid carcinoma, J Clin Endocrinol Metab **88** (2003) 1433–1441.

[16] PACINI, F., MOLINARO, E., CASTAGNA, M.G., et al., Recombinant human thyrotropin-stimulated serum thyroglobulin combined with neck ultrasonography has the highest sensitivity in monitoring differentiated thyroid carcinoma, J Clin Endocrinol Metab **88** (2003) 3668–3673.

[17] SCHLUMBERGER, M., BERG, G., COHEN, O., et al., Follow-up of low-risk patients with differentiated thyroid carcinoma: a European perspective, Eur J Endocrinol **150** (2004) 105–112.

[18] PACINI, F., SCHLUMBERGER, M., DRALLE, H., ELISEI, R., SMIT, J.W., et al., European consensus for the management of patients with differentiated thyroid carcinoma of the follicular epithelium, Eur J Endocrinol **154** (2006) 787–803.

[19] RUF, J., LEHMKUHL, L., BERTRAM, H., et al., Impact of SPECT and integrated low-dose CT after radioiodine therapy on the management of patients with thyroid carcinoma, Nucl Med Commun **25** (2004) 1177–1782.

[20] KALTSAS, G.A., BESSER, G.M., GROSSMAN, A.B., The diagnosis and medical management of advanced neuroendocrine tumors, Endocr Rev **25** (2004) 458–511.
[21] RHA, S.E., BYUN, J.Y., JUNG, S.E., et al., Neurogenic tumors in the abdomen: tumor types and imaging characteristics, Radiographics **23** (2003) 29–43.
[22] RUFINI, V., CALCAGNI, M.L., BAUM, R.P., Imaging of neuroendocrine tumors, Semin Nucl Med **36** (2006) 228–247.
[23] KRAUSZ, Y., ISRAEL, O., Single-photon emission computed tomography/computed tomography in endocrinology, Semin Nucl Med **36** (2006) 267–274.
[24] SCHILLACI, O., Hybrid SPECT/CT: a new era for SPECT imaging? Eur J Nucl Med Mol Imaging **32** (2005) 521–524.
[25] OZER, S., DOBROZEMSKY, G., KIENAST, O., et al., Value of combined XCT/SPECT technology for avoiding false positive planar ^{123}I-MIBG scintigraphy, Nuklearmedizin **43** (2004) 164–170.
[26] KEIDAR, Z., ISRAEL, O., KRAUSZ, Y., SPECT/CT in tumor imaging: technical aspects and clinical applications, Semin Nucl Med **33** (2003) 205–218.
[27] NORTON, J.A., FRAKER, D.L., ALEXANDER, H.R., et al., Surgery to cure the Zollinger-Ellison syndrome, N Engl J Med **341** (1999) 635–644.
[28] LAMBERTS, S.W.J., CHAYVIALLE, J.A., KRENNING, E.P., The visualization of gastroenteropancreatic endocrine tumors, Metabolism **41** Suppl. 2 (1992) 111–115.
[29] KRENNING, E.P., BAKKER, W.H., BREEMAN, W.A., et al., Localization of endocrine-related tumors with radioiodinated analogue of somatostatin, Lancet **1** 8632 (1989) 242–244.
[30] KRENNING, E.P., BAKKER, W.H., KOOIJ, P.P., et al., Somatostatin receptor scintigraphy with indium-111-DTPA-D-Phe-1-octreotide in men: metabolism, dosimetry and comparison with iodine-123-Tyr-3-octreotide, J Nucl Med **33** (1992) 652–658.
[31] KRENNING, E.P., KWEKKEBOOM, D.J., OEI, H.Y., et al., Somatostatin-receptor scintigraphy in gastroenteropancreatic tumors: an overview of European results, Ann NY Acad Sci **733** (1994) 416–424.
[32] SHI, W., JOHNSTON, C.F., BUCHANAN, K.D., et al., Localization of neuroendocrine tumors with [^{111}In] DTPA-octreotide scintigraphy (Octreoscan): a comparative study with CT and MR imaging, QJM **91** (1998) 295–301.
[33] WEISS, M., YELLIN, A., HUSZA'R, M., et al., Localization of adrenocorticotropic hormone-secreting bronchial carcinoid by somatostatin-receptor scintigraphy, Ann Intern Med **121** (1994) 198–199.
[34] KRENNING, E.P., KWEKKEBOOM, D.J., BAKKER, W.H., et al., Somatostatin receptor scintigraphy with [^{111}In-DTPA-D-Phe^{1}]- and [^{123}I-Tyr^{3}]-octreotide: the Rotterdam experience with more than 1000 patients, Eur J Nucl Med **20** (1993) 716–731.
[35] KWEKKEBOOM, D.J., KRENNING, E.P., Somatostatin receptor imaging, Semin Nucl Med **32** (2002) 84–91.
[36] KRAUSZ, Y., BAR-ZIV, J., DE JONG, R.B., et al., Somatostatin-receptor scintigraphy in the management of gastroenteropancreatic tumors, Am J Gastroenterol **93** (1998) 66–70.
[37] OTTE, A., MUELLER-BRAND, J., DELLAS, S., et al., Yttrium-90-labelled somatostatin-analog for cancer treatment [letter to editor], Lancet **351** (1998) 417–418.
[38] DE JONG, M., BREEMAN, W.A., BERNARD, H.F., et al., Therapy of neuroendocrine tumors with radiolabeled somatostatin-analogs, Q J Nucl Med **43** (1999) 356–366.

[39] DE JONG, M., VALKEMA, R., JAMAR, F., et al., Somatostatin receptor-targeted radionuclide therapy of tumors: preclinical and clinical findings, Semin Nucl Med **32** (2002) 133–140.
[40] LEBTAHI, R., CADIOT, G., SARDA, L., et al., Clinical impact of somatostatin receptor scintigraphy in the management of patients with neuroendocrine gastroenteropancreatic tumors, J Nucl Med **38** (1997) 853–858.
[41] LUBBERINK, M., TOLMACHEV, V., WIDSTROM, C., et al., ^{110m}In-DTPA-D-Phe^{1}-octreotide for imaging of neuroendocrine tumors with PET, J Nucl Med **43** (2002) 1391–1397.
[42] KRAUSZ, Y., SHIBLEY, N., DE JONG, R.B.J., et al., Gallbladder visualization with ^{111}In-labeled Octreotide, Clin Nucl Med **19** (1994) 133-135.
[43] CAPLIN, M.E., BUSCOMBE, J.R., HILSON, A.J., et al., Carcinoid tumor, Lancet **352** (1998) 799–805.
[44] FÖRSTER, G.J., LAUMANN, C., NICKEL, O., KANN, P., RIEKER, O., et al., SPET/CT image co-registration in the abdomen with a simple cost-effective tool, Eur J Nucl Med Mol Imaging **30** (2003) 32–39.
[45] AMTHAUER, H., RUF, J., BOHMIG, M., et al., Diagnosis of neuroendocrine tumors by retrospective image fusion: is there a benefit? Eur J Nucl Med Mol Imaging **31** (2004) 342–348.
[46] GIBRIL, F., REYNOLDS, J.C., CHEN, C.C., et al., Specificity of somatostatin receptor scintigraphy: a prospective study and effects of false-positive localizations on management in patients with gastrinomas, J Nucl Med **40** (1999) 539–553.
[47] KRAUSZ, Y., KEIDAR, Z., KOGAN, I., et al., SPECT/CT hybrid imaging with In111-pentetreotide in assessment of neuroendocrine tumors, Clin Endocrinology **59** (2003) 565–573.
[48] ALEXANDER, H.R., FRAKER, D.L., NORTON, J.A., et al., Prospective study of somatostatin receptor scintigraphy and its effect on operative outcome in patients with Zollinger-Ellison syndrome, Ann Surg **228** (1998) 228–238.
[49] ORLOFF, S.L., DEBAS, H.T., Advances in the management of patients with Zollinger- Ellison syndrome, Surg Clin North Am **75** (1995) 511–524.
[50] EVEN-SAPIR, E., KEIDAR, Z., SACHS, J., et al., The new technology of combined transmission and emission tomography in evaluation of endocrine neoplasms, J Nucl Med **42** (2001) 998–1004.
[51] PFANNENBERG, A.C., FACHMANN, S.M., HORGER, M., et al., Benefit of anatomical-functional image fusion in the diagnostic work-up of neuroendocrine neoplasms, Eur J Nucl Med Mol Imaging **30** (2003) 835–843.
[52] MIRTCHEVA, R.M., KOSTAKOGLU, L., GOLDSMITH, S.J., Hybrid imaging using ^{111}In octreotide SPECT/CT in evaluation of somatostatin receptor positive tumors (abstract), J Nucl Med **44** (2003) 73P.
[53] PALUMBO, B., SIVOLELLA, S., PALUMBO, I., et al., Ga-67 SPECT/CT with a hybrid system in the clinical management of lymphoma, Eur J Nucl Med Mol Imaging **32** (2005) 1011–1017.
[54] CARRERA, D., BAJEN, M.T., MORA, J., et al., Clinical utility of fused Ga-67 SPECT/CT scan images in patients with lymphoma, Rev Esp Med Nucl **25** (2006) 3–9.
[55] MARIANI, G., MORESCO, L., VIALE, G., et al., Radioguided sentinel lymph node biopsy in breast cancer surgery, J Nucl Med **42** (2001) 1198–1215.
[56] MARIANI, G., GIPPONI, M., MORESCO, L., et al., Radioguided sentinel lymph node biopsy in malignant cutaneous melanoma, J Nucl Med **43** (2002) 811–827.

[57] EVEN-SAPIR, E., LERMAN, H., LIEVSHITZ, G., et al., Lymphoscintigraphy for sentinel node mapping using a hybrid SPECT/CT system, J Nucl Med **44** (2003) 1413–1420.
[58] KHAFIF, A., SCHNEEBAUM, S., FLISS, D.M., et al., Lymphoscintigraphy for sentinel node mapping using a hybrid single photon emission CT (SPECT)/CT system in oral cavity squamous cell carcinoma, Head Neck **28** (2006) 874–879.
[59] LERMAN, H., METSER, U., LIEVSHITZ, G., et al., Lymphoscintigraphic sentinel node identification in patients with breast cancer: the role of SPECT/CT, Eur J Nucl Med Mol Imaging **33** (2006) 329–337.
[60] LERMAN, H., LIEVSHITZ, G., ZAK, O., METSER, U., SCHNEEBAUM, S., et al., Improved sentinel node identification by SPECT/CT in overweight patients with breast cancer, J Nucl Med **48** (2007) 201–206.
[61] MAR, M.V., MILLER, S.A., KIM, E.E., MACAPINLAC, H.A., Evaluation and localization of lymphatic drainage and sentinel lymph nodes in patients with head and neck melanomas by hybrid SPECT/CT lymphoscintigraphic imaging, J Nucl Med Technol **35** (2007) 10–16.
[62] VAN DER PLOEG, I.M., VALDES OLMOS, R.A., NIEWEG, O.E., RUTGERS, E.J., KROON, B.B., HOEFNAGEL, C.A., The additional value of SPECT/CT in lymphatic mapping in breast cancer and melanoma, J Nucl Med **48** (2007) 1756–1760.
[63] EVEN-SAPIR, E., Imaging of malignant bone involvement by morphologic, scintigraphic, and hybrid modalities, J Nucl Med **46** (2005) 1356–1367.
[64] ITO, S., KATO, K., IKEDA, M., et al., Comparison of ^{18}F-FDG PET and bone scintigraphy in detection of bone metastases of thyroid cancer, J Nucl Med **48** (2007) 889–895.
[65] HORGER, M., ESCHMANN, S.M., PFANNENBERG, C., VONTHEIN, R., BESENFELDER, H., et al., Evaluation of combined transmission and emission tomography for classification of skeletal lesions, AJR **183** (2004) 655–661.
[66] UTSUNOMIYA, D., SHIRAISHI, S., IMUTA, M., et al., Added value of SPECT/CT fusion in assessing suspected bone metastasis: comparison with scintigraphy alone and nonfused scintigraphy and CT, Radiology **238** (2006) 264–271.
[67] RÖMER, W., OLK, A., HENNIG, F.F., KUWERT, T., Assessment of aseptic loosening of the acetabular component in a total hip replacement with Tc-99m-DPD-SPECT/spiral-CT hybrid imaging, Nuklearmedizin **44** (2005) N58–N60.
[68] EVEN-SAPIR, E., FLUSSER, G., LERMAN, H., LIEVSHITZ, G., METSER, U., SPECT/multislice low-dose CT: a clinically relevant constituent in the imaging algorithm of nononcological patients referred for bone scintigraphy, J Nucl Med **48** (2007) 319–324.
[69] KAPLAN, W.D., TAKVORIAN, T., MORRIS, J.H., et al., Thallium-201 brain tumor imaging: a comparative study with pathologic correlation, J Nucl Med **28** (1987) 47–52.
[70] KIM, K.T., BLACK, K.L., MARCIANO, D., et al., Thallium-201 SPECT imaging of brain tumors: methods and results, J Nucl Med **31** (1999) 965–969.
[71] DATTA, N.R., PASRICHA, R., GAMBHIR, S., et al., Postoperative residual tumour imaged by contrast-enhanced computed tomography and Tl-201 single photon emission tomography: can they predict progression-free survival in high-grade gliomas? Clin Oncol (R Coll Radiol) **16** (2004) 494–500.
[72] LORBERBOYM, M., BARAM, J., FEIBEL, M., et al., A prospective evaluation of thallium-201 single photon emission computerized tomography for brain tumor burden, Int J Radiat Oncol Biol Phys **32** (1995) 249–254.

[73] VALLEJOS, V., BALANA, C., FRAILE, M., et al., Use of Tl-201 SPECT imaging to assess the response to therapy in patients with high grade gliomas, J Neurooncol **59** (2002) 81–90.
[74] SCOTT, A.M., MACAPINLAC, H., ZHANG, J.J., et al., Clinical applications of fusion imaging in oncology, Nucl Med Biol **21** (1994) 775–784.
[75] HEMM, S., RIGAU, V., CHEVALIER, J., et al., Stereotactic coregistration of Tl-201 SPECT and MRI applied to brain tumor biopsies, J Nucl Med **46** (2005) 1151–1157.
[76] OST, D., FEIN, A.M., FEINSILVER, S.H., Clinical practice. The solitary pulmonary nodule, N Engl J Med **348** (2003) 2535–2542.
[77] GOTTHARDT, M., BEHE, M.P., ALFKE, H., et al., Imaging lung tumors with peptide-based radioligands, Clin Lung Cancer **5** (2003) 119–124.
[78] BLUM, J., HANDMAKER, H., LISTER-JAMES, J., et al., A multicenter trial with a somatostatin analog Tc-99m depreotide in the evaluation of solitary pulmonary nodules, Chest **117** (2000) 1232–1238.
[79] HALLEY, A., HUGENTOBLER, A., ICARD, P., et al., Efficiency of ^{18}F-FDG and ^{99m}Tc-depreotide SPECT in the diagnosis of malignancy of solitary pulmonary nodules, Eur J Nucl Med Mol Imaging **32** (2005) 1026–1032.
[80] MENDA, Y., KAHN, D., Somatostatin receptor imaging of non-small cell lung cancer with Tc-99m depreotide, Semin Nucl Med **32** (2002) 92–96.
[81] DANIELSSON, R., BÅÅTH, M., SVENSSON, L., et al., Imaging of regional lymph node metastases with Tc-99m depreotide in patients with lung cancer, Eur J Nucl Med Mol Imaging **32** (2005) 925–931.
[82] MANYAK, M.J., HINKLE, G.H., OLSEN, J.O., et al., Immunoscintigraphy with In-111 capromab pendetide evaluated before definitive therapy in patients with prostate cacner, Urology **54** (1999) 1058–1063.
[83] HAN, M., PARTIN, A.W., Current applications of In-111 capromab pendetide scan, Rev Urol **3** (2001) 165–171.
[84] SCHETTINO, C.J., KRAMER, E.L., NOZ, M.E., et al., Impact of fusion of In-111 capromab pendetide volume data sets with those from MRI or CT in patients with recurrent prostate cancer, AJR **183** (2004) 519–524.
[85] SODEE, D.B., NELSON, A.D., FAULHABER, P.F., et al., Update on fused capromab pendetide imaging of prostate cancer, Clin Prostate Cancer **3** (2005) 230–238.
[86] JANI, A.B., SPELBRING, D., HAMILTON, R., et al., Impact of radioimmuonoscintigraphy on definition of clinical target volume for radiotherapy after prostatectomy, J Nucl Med **45** (2004) 238–246.
[87] KAHN, D., AUSTIN, J.C., MAGUIRE, R.T., et al., A phase II study of Y-90 capromab pendetide in the treatment of men with prostate cancer recurrence following radical prostatectomy, Cancer Biother Radiopharm **14** (1999) 99–111.
[88] MARIANI, G., GULEC, S.A., RUBELLO, D., et al., Preoperative localization and radioguided parathyroid surgery, J Nucl Med **44** (2003) 1443–1458.
[89] RUBELLO, D., PELIZZO, M.R., BONI, G., et al., Radioguided surgery of primary hyperparathyroidism using the low ^{99m}Tc-Sestamibi dose protocol: multi-institutional experience from the Italian Study Group on Radioguided Surgery and ImmunoScintigraphy (GISCRIS), J Nucl Med **46** (2005) 220–226.
[90] RUBELLO, D., GROSS, M.D., MARIANI, G., AL-NAHHAS, A., Scintigraphic techniques in hyper-parathyroidism: from pre-operative localization to intra-operative imaging, Eur J Nucl Med Mol Imaging **34** (2007) 926–933.
[91] BILLOTEY, C., SARFATI, E., AURENGO, A., et al., Advantages of SPECT in technetium-99m-sestamibi parathyroid scintigraphy, J Nucl Med **37** (1996) 1773–1778.

[92] PATTOU, F., HUGLO, D., PROYE, C., Radionuclide scanning in parathyroid disease, Br J Surg (1998) **85** 1605–1616.
[93] FRANCIS, I.S., LONEY, E.L., BUSCOMBE, J.R., THAKRAR, D.S., BERGER, L., et al., Technetium-99m-sestamibi dual-phase SPECT imaging: concordance with ultrasound, Nucl Med Commun **20** (1999) 487–488.
[94] LONEY, E.L., BUSCOMBE, J.R., HILSON, A.J.W., DAVENPORT, A., FRANCIS, I.S., Preoperative imaging of parathyroid glands, Lancet **354** (1999) 1819–1820.
[95] MOKA, D., VOTH, E., DIETLEIN, M., LAREAN-AVELLANDA, A., SCHICHA, H., Technetium 99m-MIBI-SPECT: a highly sensitive diagnostic tool for localization of parathyroid adenomas, Surgery **128** (2000) 29–35.
[96] O'DOHERTY, M.J., KETTLE, A.G., Parathyroid imaging: preoperative localization, Nucl Med Commun **24** (2003) 125–131.
[97] SPANU, A., FALCHI, A., MANCA, A., et al., The usefulness of neck pinhole SPECT as a complementary tool to planar scintigraphy in primary and secondary hyperparathyroidism, J Nucl Med **45** (2004) 40–48.
[98] RUBELLO, D., MASSARO, A., CITTADIN, S., et al., Role of ^{99m}Tc-sestamibi SPECT in accurate selection of primary hyperparathyroid patients for minimally invasive radio-guided surgery, Eur J Nucl Med Mol Imaging **33** (2006) 1091–1094.
[99] GAYED, I.W., KIM, E.E., BROUSSARD, W.F., et al., The value of ^{99m}Tc-sestamibi SPECT/CT over conventional SPECT in the evaluation of parathyroid adenomas or hyperplasia, J Nucl Med **46** (2005) 248–252.
[100] KRAUSZ, Y., BETTMAN, L., GURALNIK, L., et al., Technetium-99m-MIBI SPECT/CT in primary hyperparathyroidism, World J Surg **30** (2006) 76–83.
[101] SERRA, A., BOLASCO, P., SATTA, L., et al., Role of SPECT/CT in the preoperative assessment of hyperparathyroid patients, Radiol Med **111** (2006) 999–1008.
[102] LAVELY, W.C., GOETZE, S., FRIEDMAN, K.P., et al., Comparison of SPECT/CT, SPECT, and planar imaging with single-and dual-phase ^{99m}Tc-sestamibi parathyroid scintigraphy, J Nucl Med **48** (2007) 1084–1089.
[103] RUF, J., SEEHOFER, D., DENEKE, T., STELTER, L., RAYES, N., et al., Impact of image fusion and attenuation correction by SPECT-CT on the scintigraphic detection of parathyroid adenomas, Nuklearmedizin **46** (2007) 15–21.
[104] PIGA, M., SERRA, A., UCCHEDDU, A., LAI, L.M., FAA, G., Decisive presurgical role of MIBI SPECT/CT in identifying within a calcific thyroid nodule the parathyroid responsible for primary hyperparathyroidism, Surgery **140** (2006) 837–838.
[105] PALESTRO, C.J., TORRES, M.A., Radionuclide imaging in orthopedic infections, Semin Nucl Med **27** (1997) 334–345.
[106] LOVE, C., PALESTRO, C.J., Radionuclide imaging of infection, J Nucl Med Technol **32** (2004) 47–57.
[107] ZHUANG, H., YU, J.Q., ALAVI, A., Applications of fluorodeoxyglucose-PET imaging in the detection of infection and inflammation and other benign disorders, Radiol Clin North Am **43** (2005) 121–134.
[108] ANNOVAZZI, A., BAGNI, B., BURRONI, L., D'ALESSANDRIA, C., SIGNORE, A., Nuclear medicine imaging of inflammatory/infective disorders of the abdomen, Nucl Med Commun **26** (2005) 657–664.
[109] LOVE, C., TOMAS, M.B., TRONCO, G.G., PALESTRO, C.J., FDG PET of infection and inflammation, Radiographics **25** (2005) 1357–1368.
[110] TERMAAT, M.F., RAIJMAKERS, P.G., SCHOLTEN, H.J., BAKKER, F.C., PATKA, P., et al., The accuracy of diagnostic imaging for the assessment of chronic osteomyelitis: a systematic review and meta-analysis, J Bone Joint Surg Am **87** (2005) 2464–2471.

[111] JAMES, S.L., DAVIES, A.M., Imaging of infectious spinal disorders in children and adults, Eur J Radiol **58** (2006) 27–40.
[112] VOS, F.J., BLEEKER-ROVERS, C.P., CORSTENS, F.H., KULLBERG, B.J., OYEN, W.J., FDG-PET for imaging of non-osseous infection and inflammation, Q J Nucl Med Mol Imaging **50** (2006) 121–130.
[113] STUMPE, K.D., STROBEL, K., ^{18}F FDG-PET imaging in musculoskeletal infection, Q J Nucl Med Mol Imaging **50** (2006) 131–142.
[114] RINI, J.N., PALESTRO, C.J., Imaging of infection and inflammation with ^{18}F-FDG-labeled leukocytes, Q J Nucl Med Mol Imaging **50** (2006) 143–146.
[115] PRANDINI, N., LAZZERI, E., ROSSI, B., ERBA, P., PARISELLA, M.G., et al., Nuclear medicine imaging of bone infections, Nucl Med Commun **27** (2006) 633–644.
[116] CONCIA, E., PRANDINI, N., MASSARI, L., et al., Osteomyelitis: clinical update for practical guidelines, Nucl Med Commun **27** (2006) 645–660.
[117] LEE, E., WORSLEY, D.F., Role of radionuclide imaging in the orthopedic patient, Orthop Clin North Am **37** (2006) 485–501.
[118] EL-MAGHRABY, T.A., MOUSTAFA, H.M., PAUWELS, E.K., Nuclear medicine methods for evaluation of skeletal infection among other diagnostic modalities, Q J Nucl Med Mol Imaging **50** (2006) 167–192.
[119] PAKOS, E.E., TRIKALINOS, T.A., FOTOPOULOS, A.D., IOANNIDIS, J.P., Prosthesis infection: diagnosis after total joint arthroplasty with antigranulocyte scintigraphy with ^{99m}Tc-labeled monoclonal antibodies – a meta-analysis, Radiology **242** (2007) 101–108.
[120] PINEDA, C., VARGAS, A., RODRIGUEZ, A.V., Imaging of osteomyelitis: current concepts, Infect Dis Clin North Am **20** (2006) 789–825.
[121] MELLER, J., SAHLMANN, C.O., SCHEEL, A.K., ^{18}F-FDG PET and PET/CT in fever of unknown origin, J Nucl Med **48** (2007) 35–45.
[122] CHRISTIAN, S., KRAAS, J., CONWAY, W.F., Musculoskeletal infections, Semin Roentgenol **42** (2007) 92–101.
[123] AULER, M.A., BAGG, S., GORDON, L., The role of nuclear medicine in imaging infection, Semin Roentgenol **42** (2007) 117–121.
[124] BUNYAVIROCH, T., AGGARWAL, A., OATES, M.E., Optimized scintigraphic evaluation of infection and inflammation: role of single-photon emission computed tomography/computed tomography fusion imaging, Semin Nucl Med **36** (2006) 295–311.
[125] INGUI, C.J., SHAH, N.P., OATES, M.E., Infection scintigraphy: added value of single-photon emission computed tomography/computed tomography fusion compared with traditional analysis, J Comput Assist Tomogr **31** (2007) 375–380.
[126] BAR-SHALOM, R., YEFREMOV, N., GURALNIK, L., et al., SPECT/CT using ^{67}Ga and ^{111}In-labeled leukocyte scintigraphy for diagnosis of infection, J Nucl Med **47** (2006) 587–594.
[127] FILIPPI, L., SCHILLACI, O., Usefulness of hybrid SPECT/CT in ^{99m}Tc-HMPAO-labeled leukocyte scintigraphy for bone and joint infections, J Nucl Med **47** (2006) 1908–1913.
[128] LAZZERI, E., ERBA, P.A., PERRI, M., TASCINI, C., DORIA, R., et al., Role of one-step radiolabeled biotin SPECT/CT in the diagnosis of spinal infection, J Nucl Med **48** Suppl. 2 (2007) 280P.
[129] HORGER, M., ESCHMANN, S.M., PFANNENBERG, C., et al., The value of SPET/CT in chronic osteomyelitis, Eur J Nucl Med Mol Imaging **30** (2003) 1665–1673.

[130] GIBBONS, R.J., CHATTERJEE, K., DALEY, J., et al., ACC/AHA/ACP-ASIM guidelines for the management of patients with chronic stable angina: a report of the American College of Cardiology/American Heart Association Task Force on Practice Guidelines (Committee on Management of Patients with Chronic Stable Angina), J Amer Coll Cardiol **33** (1999) 2092–2197.
[131] VAN TRAIN, K.F., GARCIA, E.V., MADDAHI, J., et al., Multi-center trial validation for quantitative analysis of same-day rest-stress technetium-99m-sestamibi myocardial tomograms, J Nucl Med **35** (1994) 609–618.
[132] FLEISCHMANN, K.E., HUNINK, M.G.M., KUNTZ, K.M., et al., Exercise echocardiography or exercise SPECT imaging? A meta-analysis of diagnostic test performance, JAMA **280** (1998) 913–920.
[133] CORBETT, J.R., FICARO, E.P., Clinical review of attenuation-corrected cardiac SPECT, J Nucl Cardiol **6** (1999) 54–68.
[134] FRIEDMAN, T.D., GREENE, A.C., ISKANDRIAN, A.S., et al., Exercise thallium-201 myocardial scintigraphy in women: correlation with coronary arteriography, Am J Cardiol **49** (1982) 1632–1637.
[135] GOODGOLD, H.M., REHDER, J.G., SAMUELS, L.D., et al., Improved interpretation of exercise Tl-201 myocardial perfusion scintigraphy in women: characterization of breast attenuation artifacts, Radiology **165** (1987) 361–366.
[136] DESMARIAS, R., KAUL, S., WATSON, D., et al., Do false positive thallium-201 scans lead to unnecessary catheterization? Outcome of patients with perfusion defects on quantitative planar thallium scintigraphy, J Am Coll Cardiol **21** (1993) 1058–1063.
[137] HOLLY, T.A., PARKER, M.A., HENDEL, R.C., The prevalence of non-uniform soft tissue attenuation in myocardial SPECT perfusion imaging and the impact of gated SPECT, J Nucl Cardiol **4** (1997) S103 (abstract).
[138] TAN, P., BAILEY, D.L., MEIKLE, S.R., et al., A scanning line source for simultaneous emission and transmission measurements in SPECT, J Nucl Med **34** (1993) 1752–1760.
[139] GOETZE, S., BROWN, T.L., LAVELY, W.C., et al., Attenuation correction in myocardial perfusion SPECT/CT: effects of misregistration and value of re-registration, J Nucl Med **48** (2007) 1090–1095.
[140] GAEMPERLI, O., SCHEPIS, T., VALENTA, I., et al., Cardiac image fusion from stand-alone SPECT and CT: clinical experience, J Nucl Med **48** (2007) 696–703.
[141] RISPLER, S., KEIDAR, Z., GHERSIN, E., et al., Integrated single-photon emission computed tomography and computed tomography coronary angiography for the assessment of hemodynamically significant coronary artery lesions, J Am Coll Cardiol **49** (2007) 1059–1067.
[142] WIJNS, W., Anatomic-functional imaging by single-photon emission computed tomography/computed tomography as the cornerstone of diagnosis and treatment for coronary patients: a glimpse into the (near) future? J Am Coll Cardiol **49** (2007) 1068–1070.
[143] RUMBERGER, J.A., SIMONS, D.B., FITZPATRICK, L.A., et al., Coronary artery calcium area by electron-beam computed tomography and coronary atherosclerotic plaque area. A histologic correlative study, Circulation **92** (1995) 2157–2162.
[144] DANIELL, A.L., WONG, N.D., FRIEDMAN, J.D., et al., Concordance of coronary artery calcium estimates between MDCT and electron beam tomography, AJR **185** (2005) 1542–1545.
[145] VIRMANI, R., BURKE, A.P., FARB, A., et al., Pathology of the vulnerable plaque, J Am Coll Cardiol **47** Suppl. 8 (2006) C13–C18.

[146] MAHMARIAN, J.J., Hybrid SPECT-CT: integration of CT coronary artery calcium scoring and angiography with myocardial perfusion, Curr Cardiol Rep **9** (2007) 129–135.
[147] MINIATI, M., PISTOLESI, M., MARINI, C., et al., Value of perfusion lung scan in the diagnosis of pulmonary embolism: results of the Prospective Investigative Study of Acute Pulmonary Embolism Diagnosis (PISA-PED), Am J Respir Crit Care Med **154** (1996) 1387–1393.
[148] MINIATI, M., PREDILETTO, R., FORMICHI, B., et al., Accuracy of clinical assessment in the diagnosis of pulmonary embolism, Am J Respir Crit Care Med **159** (1999) 864–871.
[149] MINIATI, M., PISTOLESI, M., Assessing the clinical probability of pulmonary embolism, Q J Nucl Med **45** (2001) 287–293.
[150] MARINI, C., PALLA, A., GIUNTINI, C., Pulmonary embolism: lung scan and computed tomography, Ital Heart J **6** (2005) 811–817.
[151] PALLA, A., BARDI, G., RIBAS, C., Diagnosis of pulmonary embolism, Semin Thromb Hemost **32** (2006) 822–830.
[152] McLEAN, R.G., CAROLAN, M., BUI, C., et al., Comparison of new clinical and scintigraphic algorithms for the diagnosis of pulmonary embolism, Br J Radiol **77** 917 (2004) 372–376.
[153] THE PIOPED INVESTIGATORS, Value of the ventilation/perfusion scan in acute pulmonary embolism: results of the prospective investigation of pulmonary embolism diagnosis (PIOPED), JAMA **263** (1990) 2753–2759.
[154] SCHOEPF, J.U., GOLDHABER, S.Z., COSTELLO, P., Spiral computed tomography for acute pulmonary embolism, Circulation **109** (2004) 2160–2167.
[155] GARG, K., WELSH, C.H., FEYERABEND, A.J., et al., Pulmonary embolism: diagnosis with spiral CT and ventilation-perfusion scanning: correlation with pulmonary angiographic results or clinical outcome, Radiology **208** (1998) 201–208.
[156] GHAYE, B., SZPAIRE, D., MASTORA, I., et al., Peripheral pulmonary arteries: how far in the line does multi-detector row spiral CT allow analysis? Radiology **219** (2001) 629–236.
[157] SCHOEPF, U., HOLZKNECHT, N., HELBEREGR, T.K., et al., Subsegmental pulmonary emboli: improved detection with thin-collimation multi-detector row spiral CT, Radiology **222** (2002) 483–490.
[158] PATEL, S., KAZEROONI, E.A., CASCADE, P.N., Pulmonary embolism: optimization of small pulmonary artery visualization at multi-detector row CT, Radiology **227** (2003) 455–460.
[159] STEIN, P.D., FOWLER, S.E., GOODMAN, L.R., et al., Multidetector computed tomography for acute pulmonary embolism, N Engl J Med **354** (2006) 2317–2327.
[160] PERRIER, A., BOUNAMEAUX, H., Accuracy or outcome in suspected pulmonary embolism, N Engl J Med **354** (2006) 2383–2385.
[161] LE GAL, G., RIGHINI, M., PARENT, F., VAN STRIJEN, M., COUTURAUD, F., Diagnosis and management of subsegmental pulmonary embolism, J Thromb Haemost **4** (2006) 724–731.
[162] HARRIS, B., BAILEY, D., ROACH, P., BAILEY, E., KING, G., Fusion imaging of computed tomographic pulmonary angiography and SPECT ventilation/perfusion scintigraphy: initial experience and potential benefit, Eur J Nucl Med Mol Imaging **34** (2007) 135–142.
[163] HUTTON, B.F., BRAUN, M., THURFJELL, L., LAU, D.Y.H., Image registration: an essential tool for nuclear medicine, Eur J Nucl Med **29** (2002) 559–577.
[164] SLOMKA, P.J., Software approach to merging molecular with anatomic information, J Nucl Med **45** Suppl. 1 (2004) 36S–45S.

[165] COHADE, C., OSMAN, M., MARSHALL, L.N., WAHL, R.N., PET-CT: accuracy of PET and CT spatial registration of lung lesions, Eur J Nucl Med Mol Imaging **30** (2003) 721–726.
[166] NÖMAYR, A., RÖMER, W., HOTHORN, T., et al., Anatomical accuracy of lesion localization: retrospective interactive rigid image registration between ^{18}F-FDG-PET and X-ray CT, Nuklearmedizin **44** (2005) 149–155.
[167] WOLZ, G., NÖMAYR, A., HOTHORN, T., HORNEGGER, J., RÖMER, W., et al., Comparative anatomical accuracy of interactive and automated rigid registration between CT and FDG-PET, Nuklearmedizin **46** (2007) 43–48.
[168] KIM, J.H., CZERNIN, J., ALLEN-AUERBACH, M.S., et al., Comparison between ^{18}F-FDG PET, in-line PET/CT, and software fusion for restaging of recurrent colorectal cancer, J Nucl Med **46** (2005) 587–595.
[169] KRISHNASETTY, V., FISCHMAN, A.J., HALPERN, E.L., AQUINO, S.L., Comparison of alignment of computer-registered data sets: combined PET/CT versus independent PET and CT of the thorax, Radiology **237** (2005) 635–639.
[170] NÖMAYR, A., RÖMER, W., STROBEL, D., BAUTZ, W., KUWERT, T., Anatomical accuracy of hybrid SPECT/spiral CT in the lower spine, Nucl Med Commun **27** (2006) 521–528.
[171] ROSENTHAL, M.S., CULLOM, J., HAWKINS, W., MOORE, S.C., TSUI, B.M., et al., Quantitative SPECT imaging: a review and recommendations by the Focus Committee of the Society of Nuclear Medicine Computer and Instrumentation Council, J Nucl Med **36** (1995) 1489–1513.
[172] ZAIDI, H., HASEGAWA, B., Determination of the attenuation map in emission tomography, J Nucl Med **44** (2003) 291–315.
[173] CELLER, A., DIXON, K.L., CHANG, Z., BLINDER, S., POWE, J., et al., Problems created in attenuation-corrected SPECT images by artifacts in attenuation maps: a simulation study, J Nucl Med **46** (2005) 335–343.
[174] MASOOD, Y., LIU, Y.H., DEPUEY, G., et al., Clinical validation of SPECT attenuation correction using x-ray computed tomography-derived attenuation maps: multicenter clinical trial with angiographic correlation, J Nucl Cardiol **12** (2005) 676–686.
[175] FRICKE, E., FRICKE, H., WEISE, R., et al., Attenuation correction of myocardial SPECT perfusion images with low-dose CT: evaluation of the method by comparison with perfusion PET, J Nucl Med **46** (2005) 736–744.
[176] SCHULZ, V., NICKEL, I., NÖMAYR, A., et al., Effect of CT-based attenuation correction on uptake ratios in skeletal SPECT, Nuklearmedizin **46** (2007) 38–42.
[177] SHIRAISHI, S., TOMIGUCHI, S., UTSUNOMIYA, D., et al., Quantitative analysis and effect of attenuation correction on lymph node staging of non-small cell lung cancer on SPECT and CT, AJR **186** (2006) 1450–1457.
[178] MATSUNARI, I., BÖNING, G., ZIEGLER, S.I., et al., Effects of misalignment between transmission and emission scans on attenuation-corrected cardiac SPECT, J Nucl Med **39** (1998) 411–416.
[179] FRICKE, H., FRICKE, E., WEISE, R., KAMMEIER, A., LINDNER, O., et al., A method to remove artifacts in attenuation-corrected myocardial perfusion SPECT introduced by misalignment between emission scan and CT-derived attenuation maps, J Nucl Med **45** (2004) 1619–1625.
[180] CHEN, J., CAPUTLU-WILSON, S.F., SHI, H., GALT, J.R., FABER, T.L., et al., Automated quality control of emission-transmission misalignment for attenuation correction in myocardial perfusion imaging with SPECT-CT systems, J Nucl Cardiol **13** (2006) 43–49.

[181] BOUCEK, J., TURNER, J.H., Validation of prospective whole body bone marrow dosimetry by SPECT/CT multimodality imaging in I-131 anti-CD 20 rituximab radioimmunotherapy of non-Hodgkin's lymphoma, Eur J Nucl Med Mol Imaging **32** (2005) 458–469.
[182] SONG, H., HE, B., PRIDEAUX, A., DU, Y., et al., Lung dosimetry for radioiodine treatment planning in the case of diffuse lung metastases, J Nucl Med **47** (2006) 1985–1994.
[183] GENOVESI, D., DI MARTINO, F., LOI, A., LAZZERI, M., BONI, G., et al., Use of SPECT-CT for optimizing dosimetry estimates in patients with metastatic bone disease treated with ^{153}Sm-EDTMP, Q J Nucl Med Mol Imaging **51** (2007) 380 (abstract).
[184] RICCI, S., BONI, G., PASTINA, I., et al., Clinical benefit of bone-targeted radiometabolic therapy with ^{153}Sm-EDTMP combined with chemotherapy in patients with metastatic hormone-refractory prostate cancer, Eur J Nucl Med Mol Imaging **34** (2007) 1023–1030.
[185] O'DANIEL, J.C., STEVENS, D.M., CODY, D.D., Reducing radiation exposure from survey CT scans, AJR **185** (2005) 509–515.
[186] NUNEZ, R., ERWIN, W.D., WENDT, R.E., et al., Acquisition parameters for oncologic imaging with a new SPECT/multislice CT scanner, RadioGraphics **2007** (in review).
[187] YANG, D.J., AZHDARINIA, A., KIM, E.E., Tumor specific imaging using Tc-99m and Ga-68 labeled radiopharmaceuticals, Curr Med Imag Rev **1** (2005) 25–34.
[188] YANG, D.J., KIM, C.G., SCHECHTER, N.R., et al., Imaging with ^{99m}Tc ECDG targeted at the multifunctional glucose transport system: feasibility study with rodents, Radiology **226** (2003) 465–473.
[189] COLEMAN, R.E., DELBEKE, D., GUIBERTEAU, M.J., et al., Concurrent PET/CT with an integrated imaging system: intersociety dialogue from the joint working group of the American College of Radiology, the Society of Nuclear Medicine, and the Society of Computed Body Tomography and Magnetic Resonance, J Nucl Med **26** (2005) 1225–1239.
[190] BISCHOF DELALOYE, A., CARRIO, I., CUOCOLO, A., et al., White paper of the European Association of Nuclear Medicine (EANM) and the European Society of Radiology (ESR) on multimodality imaging, Eur J Nucl Med Mol Imaging **34** (2007) 1147–1151.
[191] GOURTSOYIANNIS, N., McCALL, I., REISER, M., et al., White paper of the European Society of Radiology (ESR) and the European Association of Nuclear Medicine (EANM) on multimodality imaging, Eur J Radiol **17** (2007) 1926–1930.

CONTRIBUTORS TO DRAFTING AND REVIEW

Mariani, G.	University of Pisa Medical School, Regional Center of Nuclear Medicine, Italy
Flotats, A.	Autonomous University of Barcelona, Nuclear Medicine Department, Spain
Israel, O.	Rambam Medical Center, Department of Nuclear Medicine, Israel
Kim, E.E.	MD Anderson Cancer Center, University of Texas, United States of America
Kuwert, T.	Universitätsklinikum Erlangen, Nuklearmedizinische Klinik, Germany

Consultants Meeting on Recent Advances on SPECT/CT,
Vienna, Austria, 25–27 June 2007